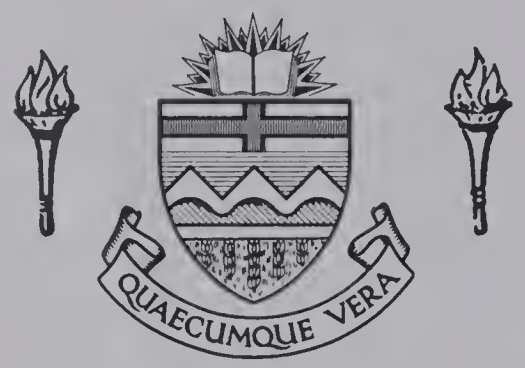

The University of Alberta
Printing Department
Edmonton, Alberta

THE UNIVERSITY OF ALBERTA

ELECTRON TUNNELING INTO SUPERCONDUCTING TIN FILMS

by

© Mohamad Abdalla EL-Semary

A THESIS

SUBMITTED TO THE FACULTY OF GRADUATE STUDIES

IN PARTIAL FULFILLMENT OF THE REQUIREMENTS FOR THE DEGREE

OF MASTER OF SCIENCE

DEPARTMENT OF PHYSICS

EDMONTON, ALBERTA

July, 1968

UNIVERSITY OF ALBERTA

FACULTY OF GRADUATE STUDIES

The undersigned certify that they have read, and recommend to the Faculty of Graduate Studies for acceptance, a thesis entitled ELECTRON TUNNELING INTO SUPERCONDUCTING TIN FILMS, submitted by Mohamad Abdalla EL-Semary in partial fulfillment of the requirements for the degree of Master of Science.

ACKNOWLEDGEMENTS

I wish to express my gratitude to Dr. S.B. Woods, my research supervisor, for his sympathetic encouragement and guidance.

I am deeply thankful to Dr. J.S. Rogers both for suggesting this project and for his constant help through the course of my research. The excellent instrumentation used in this work is only part of his total contribution.

Thanks are due to Mr. S.M. Khanna for his assistance during some of the runs.

Acknowledgements are also due to the technical staff, who supplied liquid helium and liquid air and assisted with a number of problems that were encountered.

Finally, I wish to record my thanks for the Department of Physics for providing the financial assistance.

ABSTRACT

The energy gap of Sn-Sn and Sn-Pb tunnel junctions has been measured with accuracy better than one per cent. The values of the energy gaps at 0°K are found to be $2\Delta_{Sn}(0) = 1.22$ mv and $2\Delta_{Pb}(0) = 2.6$ mv . The ratio $2\Delta_{Sn}(0)/K_BT_C \simeq 3.68$. It is experimentally confirmed that the variation of $[\Delta(T)/\Delta(0)]^2$ is a linear function of $t = T/T_c$ just below T_c, as indicated by the BCS theory. The transition temperature of Sn films is (3.83 ± 0.01)°K. The relative jump in the specific heat at T_c is calculated from the I - v traces to be (1.61 ± 0.02).

The phonon structure in Sn and Pb has been investigated at 2°K and 4.2°K respectively.

TABLE OF CONTENTS

LIST OF FIGURES

CHAPTER 1

INTRODUCTION

One of the most important facts about the nature of superconductivity is the existence of a gap in the energy spectrum of a superconductor. Many techniques are now available for measuring such a gap. Electron tunneling, discovered by Giaever (1961), is one of the most direct techniques to investigate many of the superconducting properties. This technique has been initiated in this laboratory by Adler (1962) and Rogers (1963), then extended by Penner, Khanna, and Keeler. The ultrasonic attenuation experiment is also a very useful tool to investigate the energy gap anisotropy and its temperature dependence.

This thesis contains a report of the first determination of the relative jump in electronic specific heat of Sn at the transition temperature T_c, from the current-voltage traces. This measurement might be useful especially for elements for which the electronic part is a small fraction of the total specific heat. The energy gap of Sn as a function of temperature, calculated from ultrasonic attenuation data and directly measured in an electron tunneling experiment, is compared with the BCS theory.

The electron tunneling is not a good method of exploring the anisotropic properties of the superconductor. With specimens composed of polycrystalline films, one can only obtain the average of a certain measurable quantity over the area of the tunnel junction.

CHAPTER 2

MICROSCOPIC THEORY OF SUPERCONDUCTIVITY

A. The BCS Theory

Kamerlingh Onnes (1911) investigated the temperature dependence of the electrical resistivity of a mercury sample at low temperatures. He found that at about 4°K, the resistance falls abruptly to zero. This extraordinary phenomena he called superconductivity, and the temperature at which it appears, the critical temperature T_c. Below T_c the superconducting behaviour can be quenched and normal conductivity restored by the application of an external magnetic field. It was not until (1933), that Meissner and Ochsenfeld investigated the magnetic properties of superconductors in some detail. They discovered that the magnetic induction in a superconductor vanishes (Meissner effect). The discovery of the Meissner effect was required to establish that the superconductive state is a true thermodynamic phase. In view of the Meissner effect, Gorter and Casimir (1934) were able to develop a full treatment of the superconducting phase transition. Their treatment indicates that the transition is of second order. Consequently, there is a jump in the specific heat at $T = T_c$. The magnitude of the jump is twice the electronic specific heat of the normal metal at the same temperature. Also below T_c the entropy of the superconducting phase is lower than that of the normal one, indicating that the former is the state of higher order. This ordering will later be shown to follow from a condensation of electrons in momentum

space.

Application of a magnetic field greater than H_c the critical field permits a determination of the energy difference between the normal and superconducting states. This difference, known as the condensation energy is extremely small, of the order of 10^{-8} ev per atom. Among other difficulties, this small energy difference stands as a basic one in constructing a microscopic theory for superconductivity.

A first successful theory has been developed by Bardeen, Cooper, and Schrieffer (1957); (known as BCS theory). The basis of the theory was provided by Cooper (1956) who showed that in the presence of a Fermi sea of electrons if two electrons had an energy slightly greater than the Fermi energy then in the presence of an attractive interaction they would form a bound "pair" state. BCS showed that in the presence of an attractive interaction, the electrons in the neighbourhood of the Fermi surface condense into a state of lower energy in which each electron is paired with one of opposite momentum and spin. The theory predicts the existence of an energy gap which separates the state with the largest possible number of Cooper pairs from the state with one pair less. This leads to the correct thermal and electromagnetic properties to display superconductivity.

The attraction between electrons necessary to form Cooper pairs can in principle be due to any suitable kind of interaction. The discovery by Maxwell (1950), that for many superconductors the critical temperature T_c depends on the isotopic mass, showed that for these substances the attractive interaction is one between the electrons and the lattice. The simplest way of calculating this attractive interaction is to describe it

as the emission of a virtual phonon by one electron, and its absorption by the other. Consider the processes defined in fig. (2-1), in which (a) an electron in a state $\vec{k}$ emits a phonon $\vec{q}$, and is scattered into state $\vec{k} - \vec{K}$; the electron in state $\vec{k}'$ absorbs this phonon and is scattered into $\vec{k}' + \vec{K}$. (b) A phonon $-\vec{q}$ is emitted by $\vec{K}'$, before being absorbed by $\vec{k}$. The matrix element for the transition corresponding to these processes is given by

$$(2\text{-}1) \qquad \langle \vec{k} - \vec{K},\ \vec{k}' + \vec{K} | V |\ \vec{k}, \vec{k}' \rangle = \frac{\hbar\omega_q \left| M_{\vec{k},\ \vec{k}-\vec{K}} \right|^2}{\{\varepsilon(\vec{k}) - \varepsilon(\vec{k}-\vec{K})\}^2 - (\hbar\omega_{\vec{q}})^2}$$

In this expression $M_{\vec{k},\ \vec{k}-\vec{K}}$ is the matrix element for electron-phonon interaction, $\varepsilon(\vec{k})$ is the Bloch energy of an electron in a state $\vec{k}$ measured relative to the Fermi surface, and $\hbar\omega_{\vec{q}}$ is the phonon energy, which is of the same order as the Debye energy $K_B\theta_D$. It is obvious that the interaction is attractive (negative) only for the region of energies where

$$(2\text{-}2) \qquad \left| \varepsilon(\vec{k}) - \varepsilon(\vec{k}-\vec{K}) \right| < \hbar\omega_{\vec{q}} \sim k_B\theta_D \quad ,$$

and repulsive otherwise. In this range, the matrix element for the interaction can be written as

$$(2\text{-}3) \qquad -2\,\frac{\left| M_{\vec{k},\ \vec{k}-\vec{K}} \right|^2}{\hbar\omega_{\vec{q}}} \quad .$$

The corresponding matrix element for the screened Coulomb repulsion between

Fig. (2-1) Schematic representation of electron-electron interaction by the exchange of phonons.

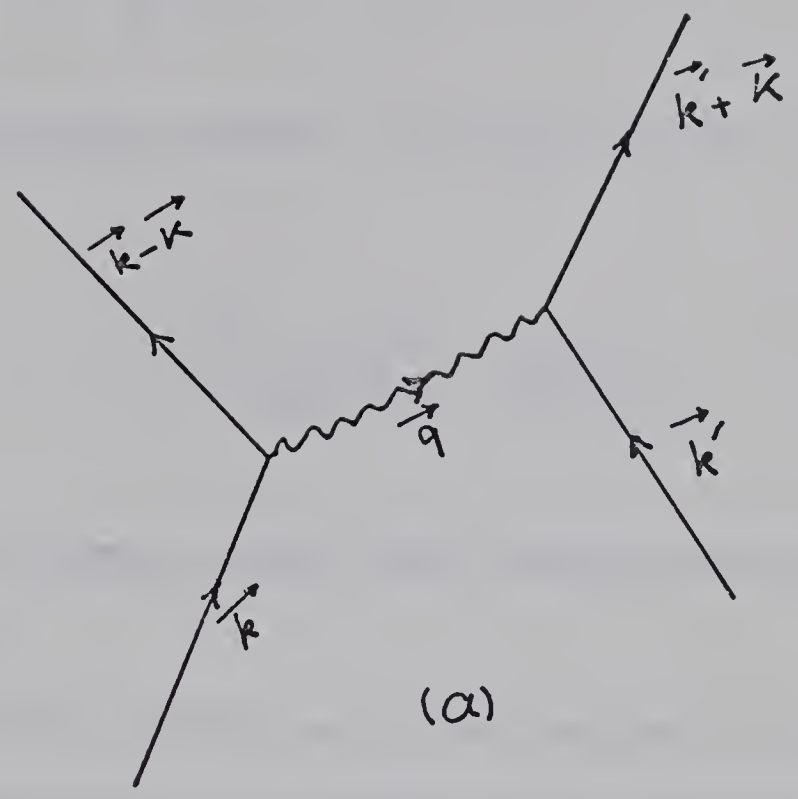
$\vec{k}+\vec{K}$
$\vec{k}-\vec{K}$
$\vec{q}$
$\vec{k}'$
$\vec{k}$

(a)

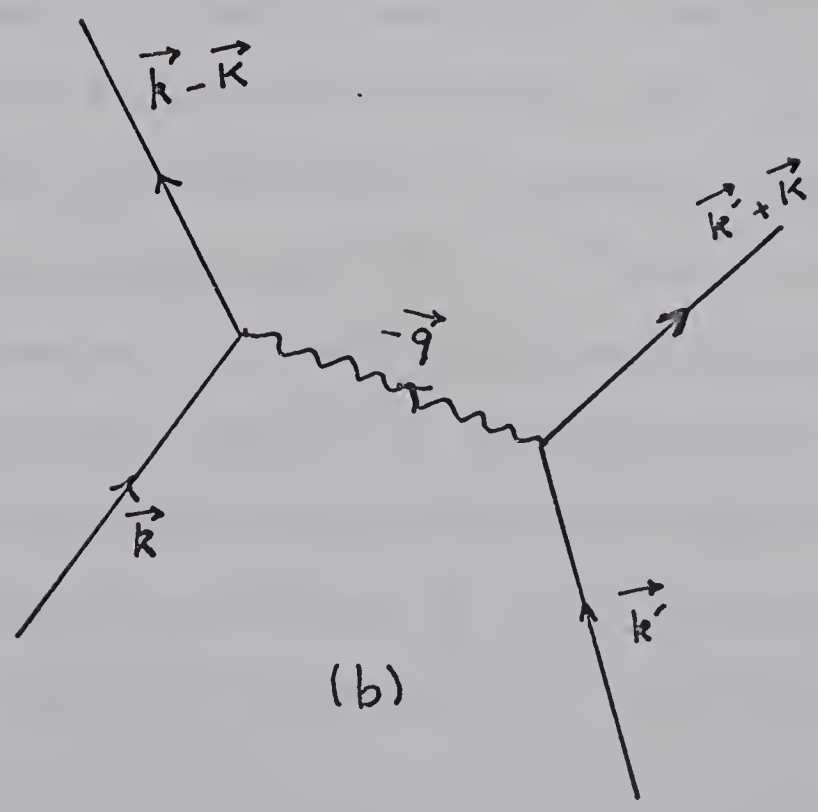
$\vec{k}-\vec{K}$
$\vec{k}'+\vec{K}$
$-\vec{q}$
$\vec{k}$
$\vec{k}'$

(b)

electrons would be

$$(2\text{-}4) \qquad \frac{4\Pi e^2}{K^2 + \lambda^2} \quad ,$$

where λ is the screening parameter. The criterion for superconductivity to occur is for

$$(2\text{-}5) \qquad -V = \left\langle -2 \frac{\left|M_{\vec{k},\,\vec{k}-\vec{K}}\right|^2}{\hbar\omega_{\vec{q}}} + \frac{4\Pi e^2}{K^2 + \lambda^2} \right\rangle$$

to be negative. The average is taken over electron states which satisfy the inequality (2-2).

Because of the Fermi statistics of the electrons, the matrix element for all possible interactions which take a pair of electrons from any two $\vec{k}$-values to any two others, alternate in sign and they are all of roughly equal magnitude. The result is a total interaction energy that is smaller than the individual terms. In order to have matrix elements of a single sign, BCS had to associate all possible $\vec{k}$ values in pairs $(\vec{k}, \vec{k}')$, and require that either both or neither member of a pair be occupied. The conservation of momentum requires that $\vec{k} + \vec{k}' = \vec{P}$ should be the same for all bound pairs. However, it is energetically most favourable to restrict the pairs to those for which $\vec{P} = 0$ and spin is zero. BCS proceed to calculate the superconducting ground state energy entirely from the correlation between paired states $(\vec{k}\uparrow, -\vec{k}\downarrow)$, by phonon and screened Coulomb interactions. A pair will be designated by a wave vector $\vec{k}$ independent of spin.

The Hamiltonian for the ground state can be expressed as

$$(2\text{-}6) \qquad H_{red} = 2 \sum_{\vec{k}} \varepsilon_{\vec{k}} b^{*}_{\vec{k}} b_{\vec{k}} - \sum_{\vec{k},\vec{k}'} V_{\vec{k}\vec{k}'} b^{*}_{\vec{k}'} b_{\vec{k}} \quad ,$$

where $$b^{*}_{k} = C^{*}_{\vec{k}\uparrow} C_{-\vec{k}\downarrow} \quad , \quad b_{\vec{k}} = C_{-\vec{k}\downarrow} C_{\vec{k}\uparrow}$$

are the creation and annihilation operators for pairs, $C^{*}_{\vec{k}\sigma}$ and $C_{\vec{k}\sigma}$ are the single electron state creation and annihilation operators, $V_{\vec{k}\vec{k}'}$ is the strength of the attractive interaction of one pair. The introduction of pair operators removes all the singly occupied states from the Hamiltonian H_{red}.

The ground state wavefunction of H_{red} is given by

$$(2\text{-}7) \qquad |\psi\rangle = \prod_{\vec{k}} (u_{\vec{k}} + v_{\vec{k}} b^{*}_{\vec{k}}) |\psi_0\rangle \quad ,$$

where $v^{2}_{\vec{k}}$ is the probability that the $\vec{k}$ th pair is occupied, $u^{2}_{\vec{k}}$ is the probability that it is not occupied, and $|\psi_0\rangle$ is the vacuum state. The normalization condition requires that

$$u^{2}_{\vec{k}} + v^{2}_{\vec{k}} = 1 \quad .$$

The condensation energy corresponding to H_{red} for the state (2-7) is

$$(2\text{-}8) \qquad W_c = 2 \sum_{\vec{k}} \varepsilon_{\vec{k}} v^{2}_{\vec{k}} - \sum_{\vec{k}\vec{k}'} v_{\vec{k}} u_{\vec{k}'} v_{\vec{k}'} u_{\vec{k}} V_{\vec{k}\vec{k}'}$$

The first term gives the difference of the kinetic energy between the

superconducting and the normal phases; the factor 2 arises because of the pairing states. This first term is smaller than the second term, which gives the correlation energy for all possible transitions from a pair state $\vec{k}$ to another $\vec{k}'$. For such a transition to be possible, $\vec{k}$ must initially be occupied and $\vec{k}'$ must be empty. The simultaneous probability of this is given by $v_{\vec{k}}^2 \, u_{\vec{k}'}^2$. The final state must have k empty and $\vec{k}'$ occupied; this has probability $v_{\vec{k}'}^2 \, u_{\vec{k}}^2$. The total correlation energy is given by the sum of the product of the matrix element $V_{\vec{k}\vec{k}'}$ by the amplitudes $v_{\vec{k}} \, u_{\vec{k}'}$ and $v_{\vec{k}'} \, u_{\vec{k}}$ over all the possible values of $\vec{k}$ and $\vec{k}'$.

The necessary condition for W_c to be minimum is

$$v_{\vec{k}}^2 = \frac{1}{2}\left(1 - \frac{\varepsilon_{\vec{k}}}{E_{\vec{k}}}\right) , \tag{2-9}$$

$$u_{\vec{k}}^2 = \frac{1}{2}\left(1 + \frac{\varepsilon_{\vec{k}}}{E_{\vec{k}}}\right) , \tag{2-10}$$

where

$$E_{\vec{k}} = (\varepsilon_{\vec{k}}^2 + \Delta_{\vec{k}}^2)^{\frac{1}{2}} , \tag{2-11}$$

and

$$\Delta_{\vec{k}} = \sum_{\vec{k}'} \frac{V_{\vec{k}\vec{k}'} \, \Delta_{\vec{k}'}}{2 E_{\vec{k}'}} \tag{2-12}$$

Figs. (2.2a) and (2.2b) illustrate equations (2-9) and (2-11) respectively.

BCS make use of the simplifying assumptions that the Fermi surface is a spherical one, and $V_{\vec{k}\vec{k}'}$ is constant for electrons in the narrow

region defined by (2-2) and vanishes elsewhere. Assuming symmetry of states on either side of the Fermi surface ($\varepsilon_F = 0$), and introducing N(0) the density of single electron states of one spin in the normal state at $\varepsilon = 0$, equation (2-12) becomes

$$\frac{1}{N(0)V} = \int_0^{\hbar\omega_{\vec{q}} \sim K_B\theta_D} \frac{d\varepsilon}{\sqrt{\varepsilon^2 + \Delta^2(0)}} \quad . \tag{2-13}$$

The limit of integration is the phonon energy above which V = 0. Equation (2-13) has a solution

$$\Delta(0) = \frac{\hbar\omega_{\vec{q}}}{\sinh 1/N(0)V} \quad . \tag{2-14}$$

For the weak coupling interaction, where $N(0)V << 1$, the gap parameter $\Delta(0)$ is given by:

$$\Delta(0) = 2\,\hbar\omega_{\vec{q}} \exp\left(-\frac{1}{N(0)V}\right) \quad . \tag{2-15}$$

The BCS energy gap parameter at 0°K is plotted in fig. (2.2c) as a function of energy ε.

At higher temperatures there is always the possibility of thermal excitations from the pair states. Because of these excitations, the number of possible pairings will be reduced, which reduces the binding energy of the system because some states will not be available for pairing interactions. This of course reduces the gap parameter $\Delta(T)$. In the BCS theory, the energy gap is defined by an implicit relation of the form

$$\frac{1}{N(0)V} = \int_0^{\hbar\omega_{\vec{q}}} \frac{\tanh[(\varepsilon^2 + \Delta^2)^{\frac{1}{2}}/2\,K_BT]}{(\varepsilon^2 + \Delta^2)^{\frac{1}{2}}}\, d\varepsilon. \tag{2-16}$$

Fig. (2-2) a - Pair occupation function $v^2_{\vec{k}}$ as given by equation (2-9).

b - Quasi-particle energy as given by equation (2-11).

c - The BCS energy gap $\Delta(0)$ as a function of energy ε_k.

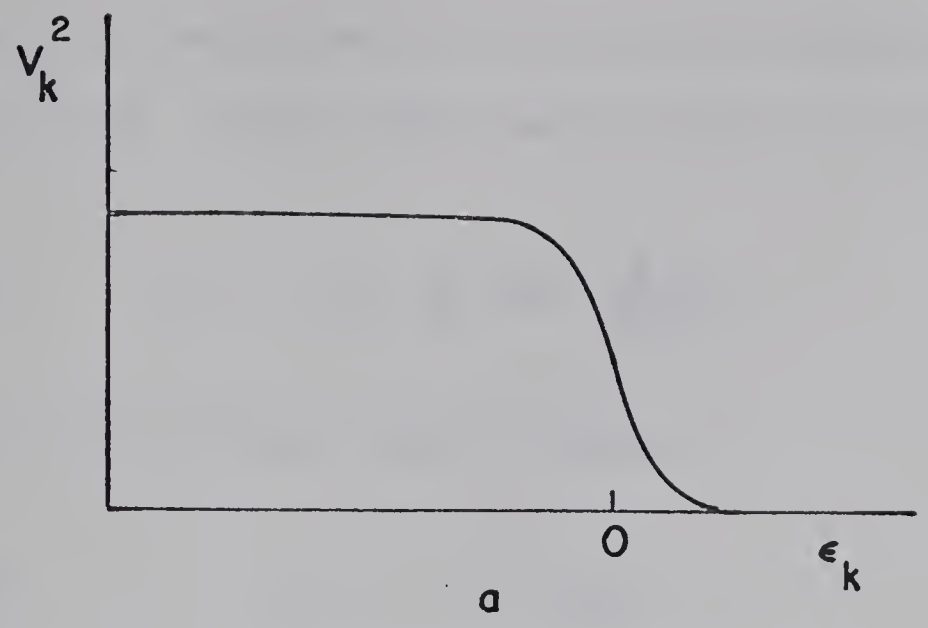
V_k^2
0
ϵ_k

a

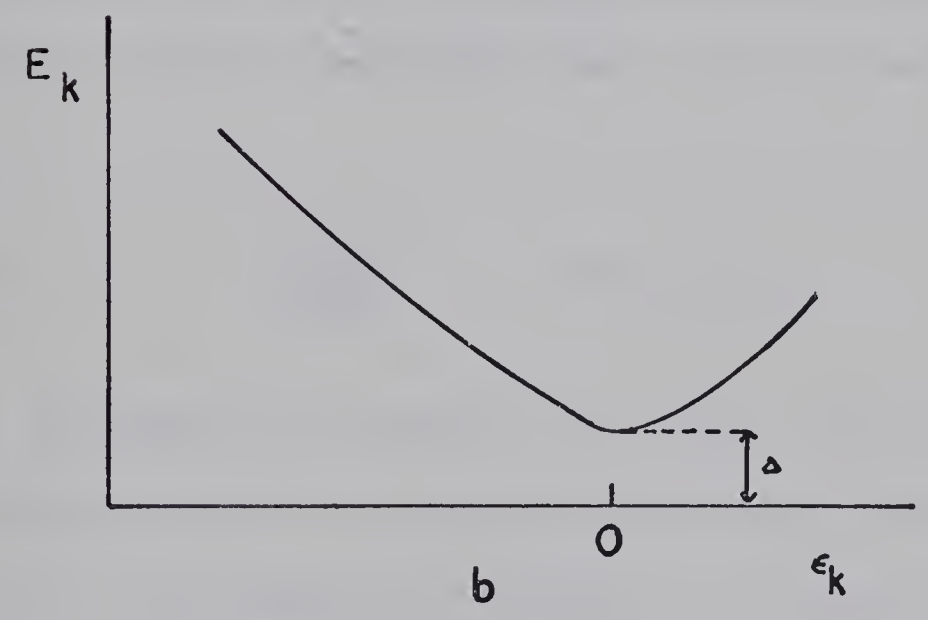
E_k
Δ
0
ϵ_k

b

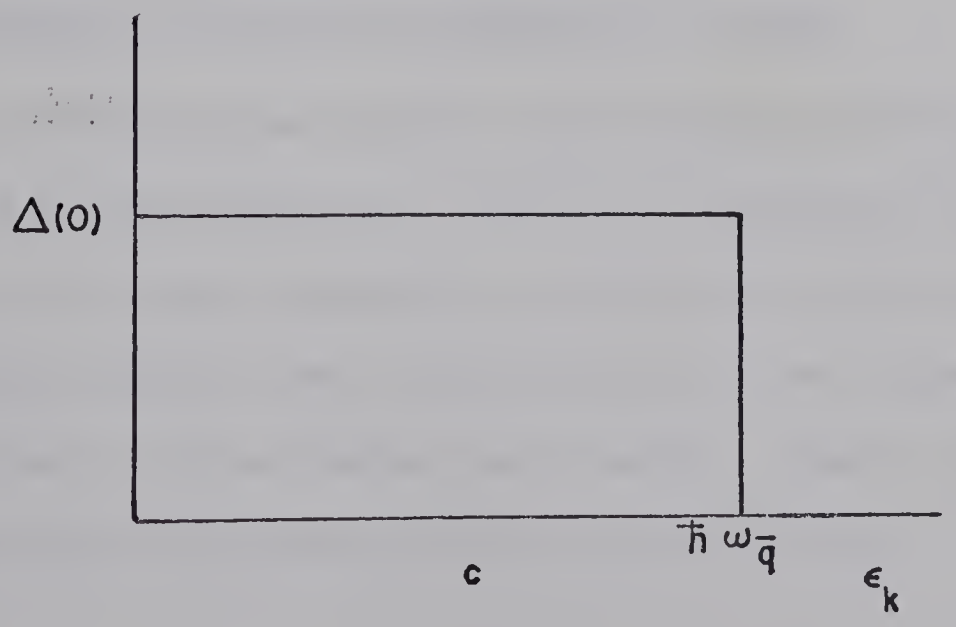
$\Delta(0)$
$\hbar\omega_{\vec{q}}$
ϵ_k

c

The transition temperature T_c is obtained by setting Δ equal to zero in equation (2-16). In the weak coupling limit this gives

$$T_c = 1.14\ \theta_D \exp\left(-\frac{1}{N(0)V}\right) \quad . \tag{2-17}$$

At T = 0°K, the half-gap can be written as

$$\Delta(0) = 1.76\ K_B T_c \quad . \tag{2-18}$$

The gap is not expressible as a function of temperature in an explicit form over most of the temperature range. Just below T_c, however, we have

$$\left[\frac{\Delta(T)}{\Delta(0)}\right]^2 \simeq -3.03\ (1-t), \tag{2-19}$$

where t is known as the reduced temperature. The gap has been tabulated over the whole temperature range by Mühlschlegel (1959) from a numerical calculation. The temperature dependence of the gap is shown in fig. (2.3).

B. Elementary Excitations and Density of States

The BCS formalism requires that the Bloch electrons in a metal be replaced by quasi-particles, which are excitations from the ground state. These are not exact eigenstates of the system, since the Hamiltonian for the system involves their interactions with each other and with other excitations, such as phonons and plasmons. However, they may be treated as approximate eigenstates with a finite lifetime.

Fig. (2-3) Temperature dependence of the energy gap.

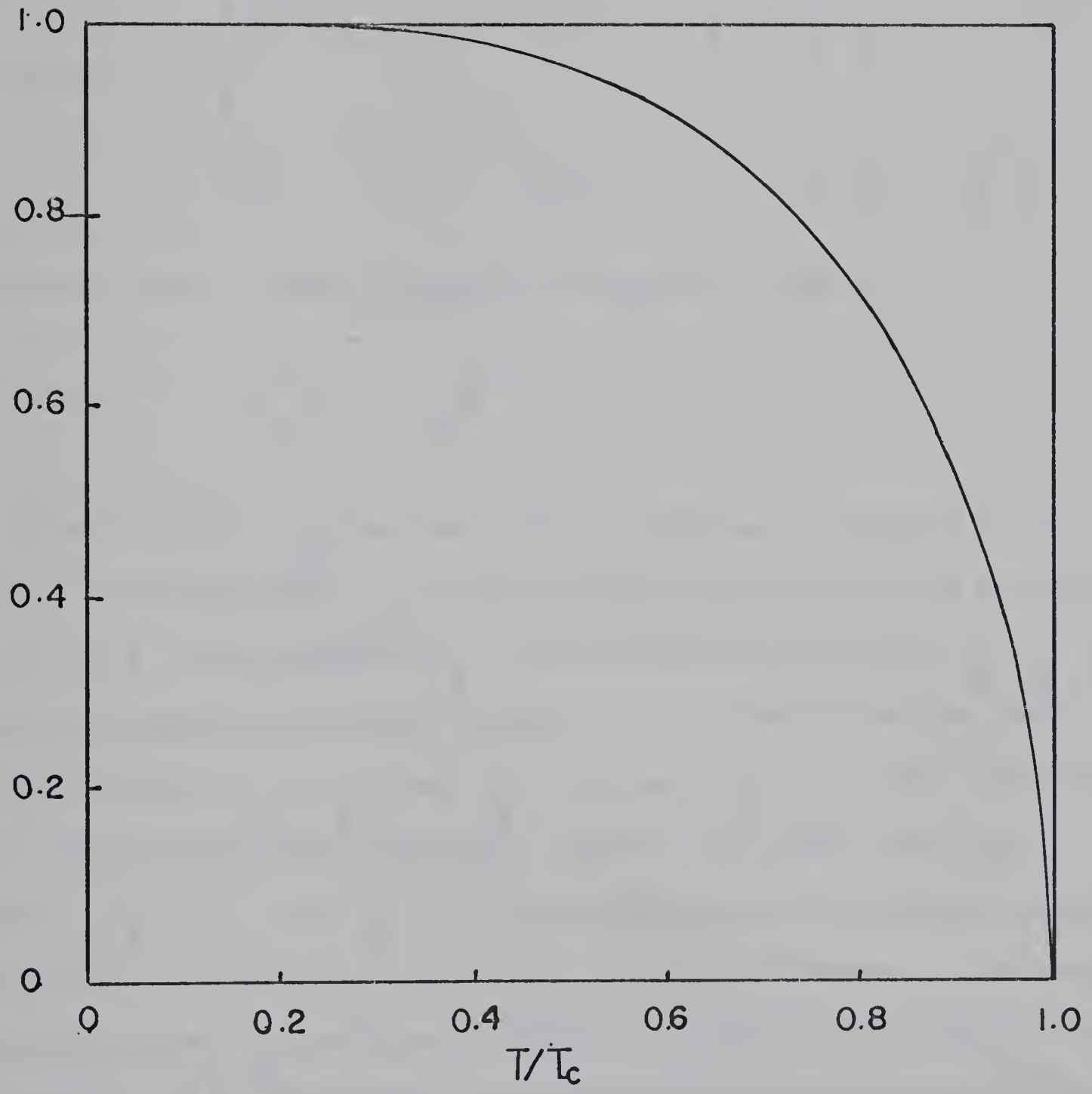
1·0
0·8
0·6
0·4
0·2
0
Δ/Δ(0)
0
0.2
0.4
0.6
0.8
1.0
T/Tc

Bogoliubov (1958) developed an equivalent theory to BCS. He introduced another set of operators formed from the annihilation and creation operators c_k, c_k^*, by a canonical transformation. This new set is

$$(2\text{-}20)\qquad \begin{cases} \gamma^*_{\vec{k}} = u_{\vec{k}}\, c^*_{\vec{k}} - v_{\vec{k}}\, c_{\vec{k}}\,, \quad \gamma_{\vec{k}} = u_{\vec{k}}\, c_{\vec{k}} - v_{\vec{k}}\, c^*_{-\vec{k}}\,, \\ \gamma^*_{-\vec{k}} = u_{\vec{k}}\, c^*_{-\vec{k}} + v_{\vec{k}}\, c_{\vec{k}}\,, \quad \gamma_{-\vec{k}} = u_{\vec{k}}\, c_{-\vec{k}} + v_{\vec{k}}\, c^*_{\vec{k}}\,. \end{cases}$$

The vacuum state of these operators is uniquely defined by

$$(2\text{-}21)\qquad \gamma_{\vec{k}}|0\rangle = \gamma_{-\vec{k}}|0\rangle = 0$$

According to (2-20) $\gamma^*_{\vec{k}}$ has the effect of creating an electron in the state $\vec{k}$, with amplitude $u_{\vec{k}}$, and at the same time destroying an electron in state $-\vec{k}$ with amplitude $v_{\vec{k}}$. The probability amplitudes $u_{\vec{k}}$, $v_{\vec{k}}$ are defined by equations (2-9) and (2-10). If k is well above the Fermi surface, so that $\varepsilon_{\vec{k}} >> \Delta_{\vec{k}}$, then $u^2_{\vec{k}} = 1$ and $v^2_{\vec{k}} = 0$. The excitation will look like an ordinary electron. However, well below the Fermi surface, $v^2_{\vec{k}} = 1$ and $u^2_{\vec{k}} = 0$; the excitation now corresponds to the destruction of an electron $-\vec{k}$, i.e. to a hole. In between, in the range of energy around $\Delta_{\vec{k}}$, each quasi-particle is a mixture of an electron in $\vec{k}$ and a hole in $-\vec{k}$. The energy of the quasi-particle in the state $\gamma^*_{\vec{k}}|0\rangle$ is $E_{\vec{k}}$, and its energy in the state $\gamma^*_{-\vec{k}}\gamma^*_{\vec{k}}|0\rangle$ is $2E_{\vec{k}}$, where $E_{\vec{k}}$ is defined by equation (2-11). The minimum energy of an allowed excitation is 2Δ, because excited single particles can only be produced in pairs.

There are no energy states available in the energy gap. Therefore the number of states in an element of energy dE is the same as that in dε, and one can write

$$(2\text{-}22) \qquad N_s(E)dE = N_n(\varepsilon)d\varepsilon \; ;$$

where $N_s(E)$ and $N_n(\varepsilon)$ are the density of states of the superconducting and normal phases respectively. Using equation (2-11), the density of superconducting state is

$$(2\text{-}23) \qquad N_s(E) = \frac{N_n(\varepsilon)\ |E|}{(E^2 - \Delta^2)^{\frac{1}{2}} + \Delta \frac{d\Delta}{d\varepsilon}} \; .$$

The BSC constant energy gap model, namely,

$$\Delta(\varepsilon) = \text{constant for } |\varepsilon| < \hbar\omega_q$$

$$= 0 \quad \text{otherwise,}$$

simplifies the expression for $N_s(E)$ to

$$(2\text{-}24) \qquad N_s(E) = N(0) \frac{|E|}{(E^2 - \Delta^2)^{\frac{1}{2}}} \quad \text{for } |E| \geq \Delta$$

$$= 0 \quad \text{for } |E| < \Delta \quad ,$$

where $N_n(\varepsilon)$ is replaced by N(0). Equation (2-24) is illustrated in fig. (2.4). Notice that $N_s(E)$ has infinite singularities at $E = \pm \Delta$, and for $E >> \Delta$, $N_s(E) = N(0)$, the density of states of one spin in the normal metal at the Fermi energy.

Fig. (2-4) The BCS density of states in a superconductor.

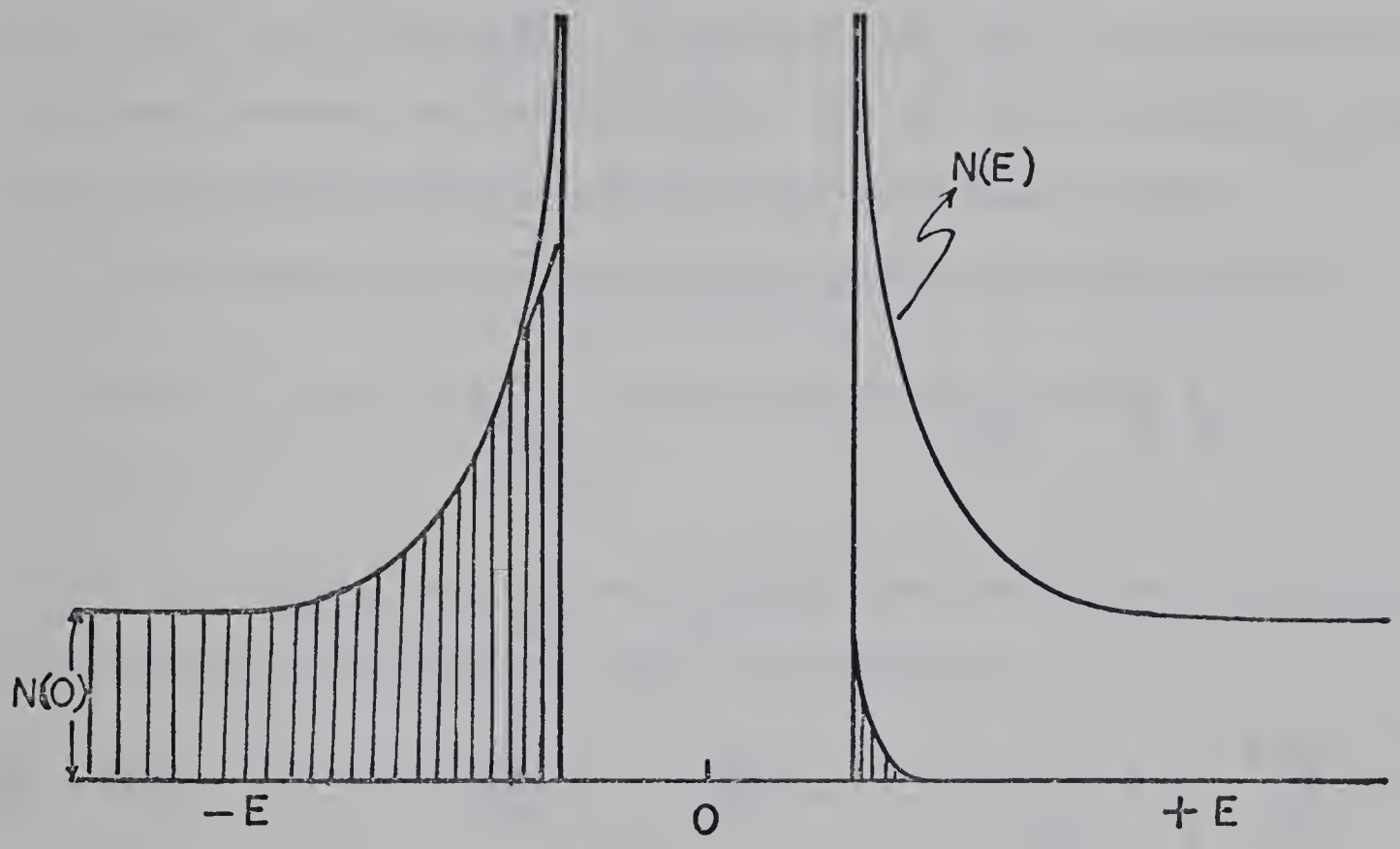
N(E)
N(O)
−E
O
+E

C. Thermodynamic Properties

For a metal in the superconducting state it is customary to separate the total specific heat, C_s, into a lattice contribution $C_{\ell s}$ and an electronic contribution C_{es}. The lattice part is assumed to take the same values in the normal and superconducting states. Early measurements of the electronic specific heat gave $C_{es} \propto T^3$, in agreement with the Gorter and Casimir two fluid model. Deviations from the T^3 law were first observed by Brown, Zemansky and Boorse (1953). The BCS theory predicts an exponentially decreasing electronic specific heat as T tends to 0°K.

The entropy in the superconducting state may be expressed as

$$(2\text{-}25) \qquad S = 4 K_B \sum_{\vec{k}>\vec{k}_F} [\ln \{1 + \exp(-\beta E_{\vec{k}})\} + \beta E_{\vec{k}} f_{\vec{k}}] \quad ,$$

where $\beta = \frac{1}{K_B T}$, and $f_{\vec{k}}$ is the Fermi function for the quasi-particles. The electronic specific heat can be expressed as

$$(2\text{-}26) \qquad C_{es} = T \frac{dS}{dT} = -\beta \frac{dS}{d\beta} = -4 K_B \beta \sum_{\vec{k}>\vec{k}_F} \beta E_{\vec{k}} \frac{d f_{\vec{k}}}{d\beta} \quad ,$$

or

$$(2\text{-}27) \qquad C_{es} = 4 K_B \beta^2 \sum_{\vec{k}>\vec{k}_F} f_{\vec{k}} (1-f_{\vec{k}}) [E_{\vec{k}}^2 + \frac{\beta}{2} \frac{d}{d\beta} (\Delta^2)] \quad .$$

The expression for C_{es} is interpreted as the specific heat due to electrons and holes with the modified spectrum

$$E_{\vec{k}} = (\varepsilon_{\vec{k}}^2 + \Delta_{\vec{k}}^2)^{\frac{1}{2}} \quad ,$$

and the appropriate change in the condensation energy with temperature. At sufficiently low temperatures for which $2\Delta(T) >> K\ T_c$, the ratio $C_{es}/\gamma T_c$ is given by

$$(2\text{-}28) \qquad \frac{C_{es}}{\gamma T_c} = \frac{3}{2\Pi^2}\left(\frac{\Delta(T)}{K_B T_C}\right)^3\left(\frac{T_c}{T}\right)^2 \left\{3\ \chi_1\left(\frac{\Delta(T)}{K_B T_C}\right) + \chi_3\left(\frac{\Delta(T)}{K_\beta T_c}\right)\right\} ,$$

where χ_1 and χ_3 are first and third order modified Bessel functions of the second kind. Equation (2-28) can be written in the form

$$(2\text{-}29) \qquad \frac{C_{es}}{\gamma T_c} \simeq 8.5 \exp\ (-\ 1.44\ T_c/T) \qquad 2.5 < T_c/T < 6$$

$$\simeq 26 \exp\ (-\ 1.62\ T_c/T) \qquad 7 < T_c/T < 11.$$

At the transition temperature, the jump in the specific heat, $C_{es} - \gamma T|T_c$ is given by

$$(2\text{-}30) \qquad K_B N(0)\ \beta^2\ \frac{d\Delta^2}{d\beta}\ |T_c$$

The derivative $d\Delta^2/d\beta$ can be obtained from the relation (2-19), between Δ and T. The BCS calculation gives the value $1.43\ \gamma T_c$ for the jump in the specific heat, while the Gorter and Casimir model gives $2\ \gamma T_c$.

Swihart (1962) solved the BCS integral equation (2-12) numerically for non-separable interactions of a form more closely related to that derived by Fröhlich (1952) and by Bardeen and Pines (1955). The effect of the Coulomb interaction was also included. It was possible to calculate the specific heat and the other thermodynamic functions in the same way as in BCS theory with the modification that the energy gap is a function of both energy and temperature. He showed that

$$(2\text{-}31) \qquad \frac{C_{es}}{\gamma T_c} = \frac{C_{es}^{(1)}}{\gamma T_c} + \frac{C_{es}^{(2)}}{\gamma T_c} \quad ,$$

where $C_{es}^{(1)}$ depends on the temperature dependence of the distribution of quasi-particles with constant energy gap, and goes to γT_c as T tends to T_c. $C_{es}^{(2)}$ depends on the temperature dependence of $\Delta(0,T)$ multiplied by a factor which is energy dependent. The factor was found to be one half in the case of weak coupling and the result is

$$(2\text{-}32) \qquad \frac{\Delta C}{\gamma T_c}\Big|_{T_c} = \frac{3}{2\Pi^2} \frac{d}{dt}\left(\frac{\Delta(0,T)}{K_B T_c}\right)^2 \quad .$$

In the case of strong coupling the factor was about 0.58, which indicates that the jump in specific heat at T_c is larger. However, this increase is not large enough to explain the results for lead. In all the treatments discussed so far, an isotropic energy gap model was considered. The anisotropy of the energy gap will be discussed below.

D. Anisotropy of the Energy Gap

Anisotropy of the gap is well shown up in ultrasonic attenuation experiments in specimens with a long mean free path. Results of experiments require a half-gap of the form

$$(2\text{-}33) \qquad \Delta(0) = C K_B T_c \quad ,$$

where C is a function of the electron wave vector $\vec{k}$. Pokrovskii (1961) proposed a model in which he assumed an effective electron-electron inter-

action that depends only on the direction of the electron k-vector. He was able to show in the weak coupling approximation that:

a) A change in temperature leads to a change in the magnitude of the gap by a factor which is independent of the direction.

b) The minimum value of the gap at T = 0°K divided by the critical temperature T_c should be less than the BCS value.

c) The change in thermodynamic quantities is qualitatively the same as in the isotropic case; however the relative jump in the specific heat at T_c is less than the BCS value.

The experiments show that the relative jump in specific heat is higher even than the BCS value. Pokrovskii and Ryvkin (1962) were able to predict the general effect of angular variations of the energy gap. A more complete theory was derived by Bennett (1965) who assumed that the strongest source of gap anisotropy is the phonon spectrum. His calculation is important in suggesting that the temperature dependence for the gap agrees with BCS.

The BCS expression for the ratio of accoustic attenuation in an isotropic superconductor to that in a normal metal is given by

$$\frac{\alpha_s}{\alpha_n} = 2 f (\Delta/K_B T) \quad , \tag{2-34}$$

where f is the Fermi function. In the anisotropic superconductor Pokrovskii found that

$$\frac{\alpha_s}{\alpha_n} = C(T/T_c)^{\frac{1}{2}} \exp (- \Delta_{min}/K_B T) \quad , \tag{2-35}$$

where Δ_{min} is the minimum value of the gap on the curve defined by

$\vec{v}.\vec{q} = 0$ on the Fermi surface. $\vec{q}$ is the momentum of the sound wave and v is the Fermi velocity. Equation (2-35) has the same temperature dependence as that of BCS theory.

Another method of observing the anisotropy is by means of tunneling experiments, which will be discussed in the next chapter.

CAHPTER 3

ELECTRON TUNNELING

A. Tunneling Theories

The most direct measurement of the energy gap has been provided by the work with tunnel junctions initiated by Giaever (1961). A tunnel junction is composed of two metallic films (1 and 2), separated by a thin insulator. The action of the insulator is to produce a potential barrier between the metallic films, which impedes the flow of electrons between them. The barrier is assumed to be thin enough to permit electron penetration by quantum-mechanical tunneling.

The matrix element $M_{\vec{k}\vec{k}'}$ for a transiton of an electron from a state $\vec{k}$ in metal 1 to a state $\vec{k}'$ in metal 2 by an applied voltage V is assumed to be constant and the same in the superconducting and the normal states. With this assumption, the probability of a transition per unit time is

$$P_{1-2}^{\vec{k}} = \frac{2\pi}{\hbar} \sum_{\vec{k}'} |M_{\vec{k}\vec{k}'}|^2 f(\varepsilon_{\vec{k}})[1 - f(\varepsilon_{\vec{k}'} + V)] \delta(\varepsilon_{\vec{k}} - \varepsilon_{\vec{k}'}) \quad . \tag{3-1}$$

In this expression $f(\varepsilon_{\vec{k}})[1 - f(\varepsilon_{\vec{k}'} + V)]$ is the probability that the initial state $\vec{k}$ is occupied and the final state $\vec{k}'$ is empty simultaneously. The net tunneling current I is then given by

$$e \sum_{\vec{k}} (P_{1-2}^{\vec{k}} - P_{2-1}^{\vec{k}}) \quad . \tag{3-2}$$

If the density of electron states is constant, and is given by its value at the Fermi surface $N(0)$, when the metal is in the normal state; and is equal to that of the BCS expression (2-24) when the metal becomes superconducting, then the summation (3-2) may be transformed to

$$(3\text{-}3) \qquad I = C \int_{-\infty}^{\infty} d\varepsilon \, \rho_1(\varepsilon)\rho_2(\varepsilon+v) \, [f(\varepsilon) - f(\varepsilon+v)] \quad ,$$

where

$$C = \frac{2\Pi}{\hbar} |M_{12}|^2 \, N_{1n}(0) \, N_{2n}(0) \quad ,$$

and $\rho_i(\varepsilon)$ is known as the reduced density of states. It is unity for the normal metal and is given by,

$$(3\text{-}4) \qquad \rho_s = \frac{|\varepsilon|}{\sqrt{\varepsilon^2 + \Delta^2}} \qquad \text{for} \quad |\varepsilon| \geq \Delta$$

$$= 0 \qquad \text{for} \quad |\varepsilon| < \Delta \quad ,$$

for a superconductor; n and s refer to the normal and the superconducting states respectively.

The following three cases are to be considered:

(1) I_{nn} ; both metals are in their normal states.

The temperature of the junction and the applied voltage are such that $K_B T \ll \varepsilon_f$ and $V \ll \varepsilon_f$. Under these conditions, the tunneling current I_{nn} can be written as

$$(3\text{-}5) \qquad C \int_{-\infty}^{\infty} \left(-\frac{\partial f}{\partial \varepsilon}\right) V d\varepsilon = CV.$$

Fig. (3-1a) illustrates the densities of electron states in two normal

metals at non zero temperature along with the I-V characteristic.

(2) I_{sn} ; metal 1 only in its superconducting state.

In this case the reduced density of states of metal 2 is unity, and that of the superconductor is given by the BCS reduced density of states. The current I_{sn} at 0°K is given by

$$(3\text{-}6) \qquad C \int_{-V}^{0} \rho_{1s}(\varepsilon)\, d\varepsilon = C(V^2 - \Delta_1^2)^{\frac{1}{2}}, \quad |V| \geq \Delta_1$$

$$= 0, \quad |V| < \Delta_1 .$$

The limit of integration is now from (-V to 0), because of the cut off in the Fermi factor at 0°K. For higher temperatures, the solution for the current I corresponding to the potential region $|V| < \Delta_1$ is given by

$$(3\text{-}7) \qquad I_{sn} = 2\, C\, \Delta_1 \sum_{m=1}^{\infty} (-1)^{m-1}\, \chi_1\left(\frac{m\Delta_1}{K_B T}\right)\, \sinh\left(\frac{mV}{K_B T}\right),$$

where χ_1 is the modified Bessel function of the second kind. The density of states and the I-V characteristic are shown in fig. (3.1b). Notice that for $T \neq 0°K$, there is a small current for $V < \Delta_1$ due to the thermally excited electrons which can tunnel into the other metal.

(3) I_{ss} ; both metals are superconductors.

The most interesting experiments are those in which the two films are different metals. A typical set of investigations was that made on Al-Pb junctions by Giaever (1961).

At zero temperature, there will be no current until the applied voltage corresponds to $\Delta_1 + \Delta_2$. At this voltage, the current increases

very sharply until it approaches I_{nn}. When the temperature is different from zero, there will be a net flow of current from metal 2 to metal 1, if a small positive voltage is applied to metal 1. As the left edges of the two gaps come into coincidence at $V = \Delta_2 - \Delta_1$, there will be an increase in current. This occurs because at the temperature of the experiment there are still a considerable number of vacant states in the lower band of metal 1 which would not exist at 0°K. As soon as the voltage is increased further, the current drops because there are now few states available. This continues until a stage is reached when the right hand band of 1 coincides with the left hand band edge of 2 at which $V = \Delta_1 + \Delta_2$. Beyond this, the current starts to increase again. The density of states as well as the I-V characteristics are shown in fig. (3.1c).

Cohen, Falicov, and Phillips (1962) have discussed tunneling of electrons in a superconductor-normal junction on the basis of an effective Hamiltonian,

$$H = H_n + H_s + H_T \quad , \tag{3-8}$$

where H_n and H_s are exact Hamiltonians for the normal and superconducting metals, respectively, and H_T is an operator which transfers electrons from one metal to the other:

$$H_T = \sum_{\vec{k},\vec{q},\sigma} \left(T_{\vec{k}\vec{q}} \, C^*_{\vec{k}\sigma} \, C_{\vec{k}\sigma} + T_{\vec{k}\vec{q}} \, C_{\vec{q}\sigma} \, C^*_{\vec{k}\sigma} \right) . \tag{3-9}$$

Here $\vec{k}$ and $\vec{q}$ refer to states in normal and superconducting metals, σ is the spin and C's are creation and annihilation operators for usual quasi-particle states in both metals. By making use of the equation of motion,

Fig. (3-1) The density of states near the Fermi level along with the I-V characteristics of

a) normal-normal case

b) normal-superconductor case

c) superconductor-superconductor case.

$T = 0^\circ K$

$T > 0^\circ K$

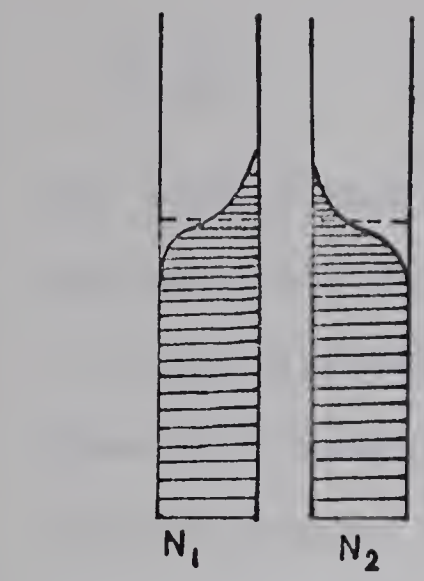

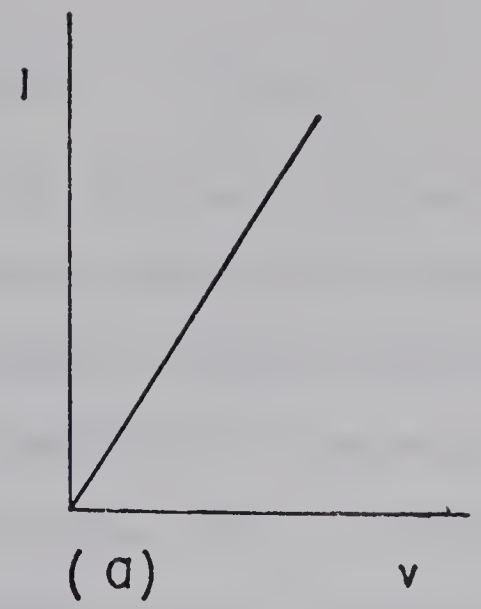

(a)

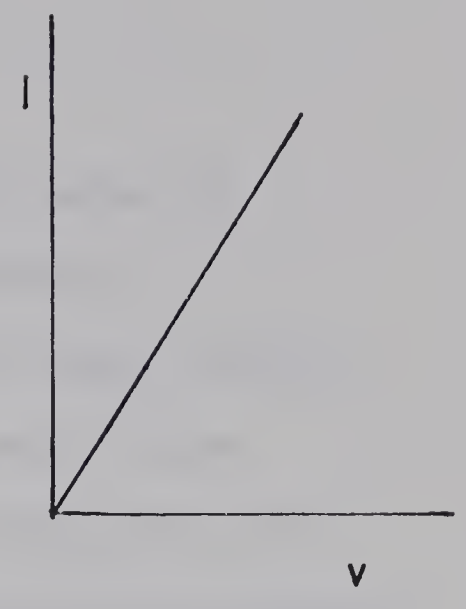

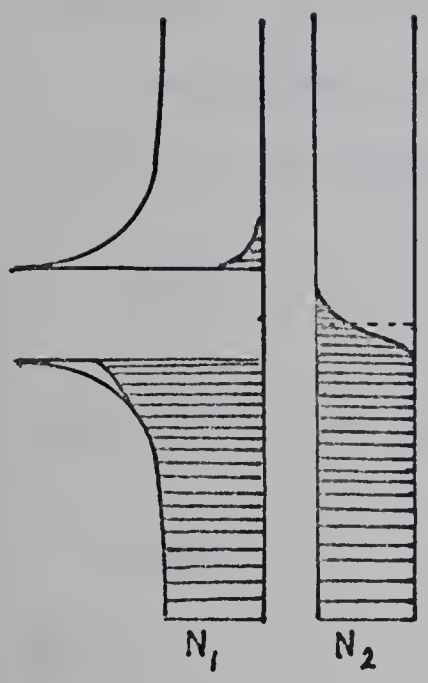

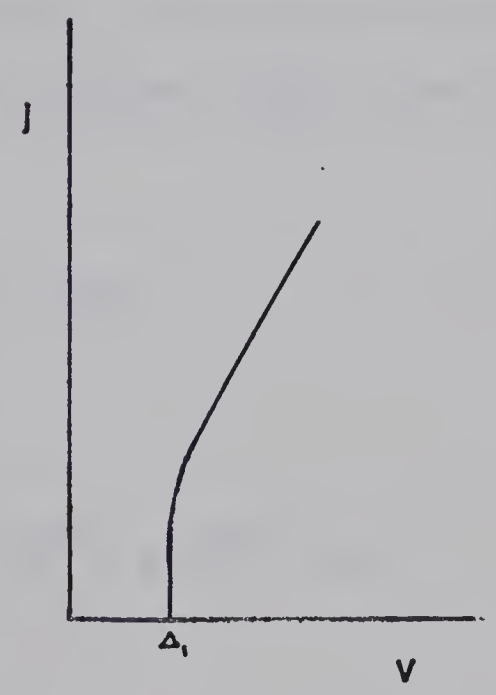

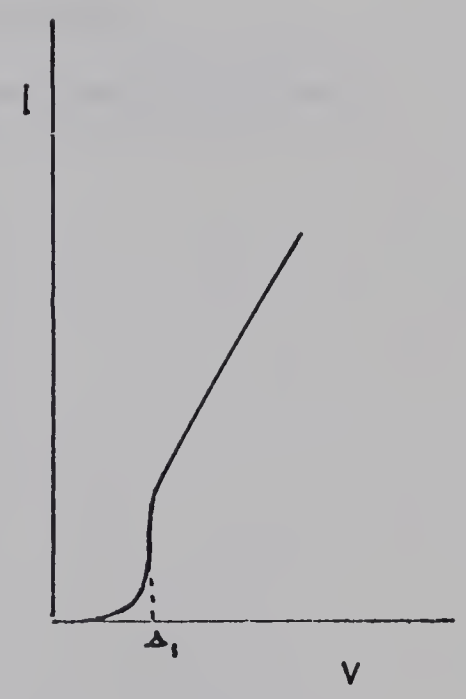

(b)

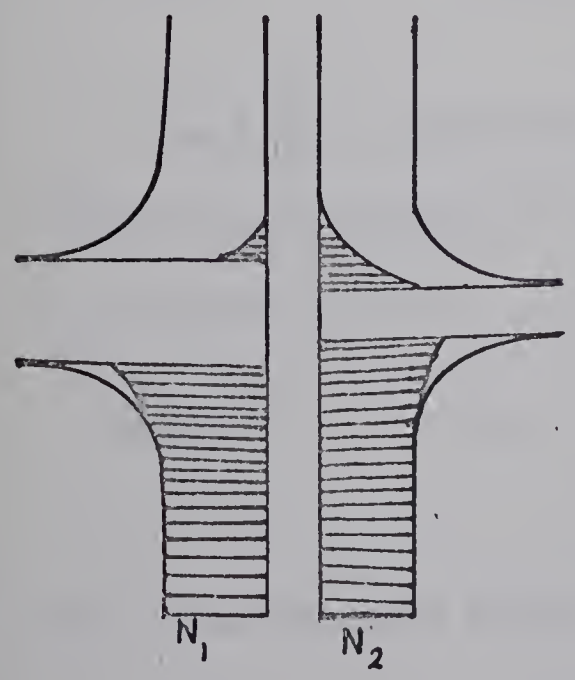

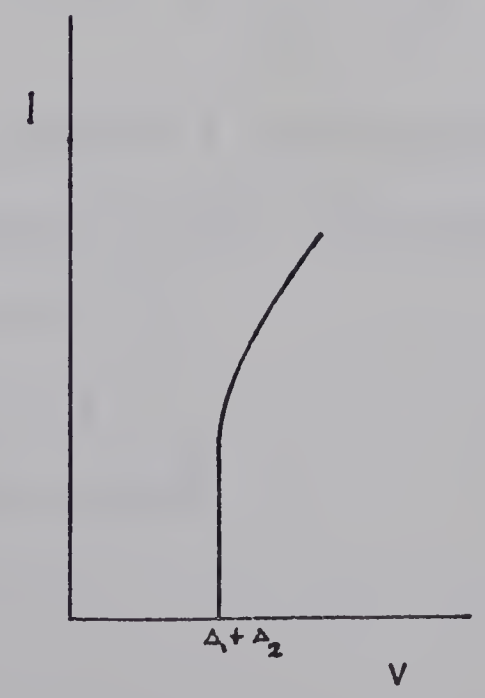

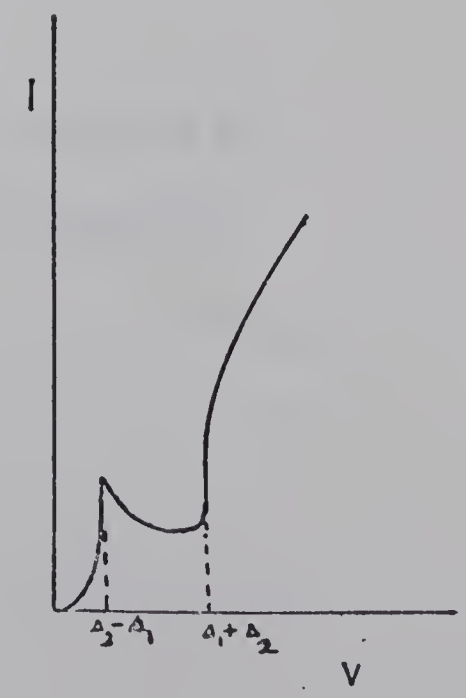

(c)

$$(3\text{-}10) \qquad i\hbar\dot{N} = [N_S, H] = [N_S, H_T] \quad ,$$

they found an expression for the time rate of change of the number of electrons, and thus the tunneling current in the superconductor.

When this theory is extended to the two superconductor case, complications arise because of the omission of the Cooper-pair transfer terms which are present in the microscopic theory. Josephson (1962) and others have shown that a proper treatment leads to additional terms in the tunneling current. These terms give rise to the so-called Josephson effect.

Schrieffer, Scalapino and Wilkins (1963) treated H_T as a small perturbation on the Hamiltonian

$$(3\text{-}11) \qquad H_0 = H_n + H_s \quad .$$

They derived the expression

$$(3\text{-}12) \qquad I \propto \int_0^V N_T^{(2)}(E)\, N_T^{(1)}(E-V)\, d\varepsilon \quad ,$$

where

$$(3\text{-}13) \qquad N_T(E) = N(0)\ RP \frac{E}{(E^2 - \Delta^2)^{\frac{1}{2}}} \quad .$$

The dynamic conductance dI/dV of a tunnel junction is obtained by taking the derivative of equation (3-12). The normalized conductance $\sigma = (dI/dV)S/(dI/dV)_n$ is found to be

$$(3\text{-}14) \qquad RP \frac{V}{(V^2 - \Delta^2(V))^{\frac{1}{2}}} \quad .$$

Since from equation (3-13)

$$N_T(V) = N(0) \frac{V}{[V^2 - \Delta^2(V)]^{\frac{1}{2}}} \quad , \tag{3-15}$$

the measurement of σ versus v will give detailed information on the superconducting tunneling density of states as a function of energy. This will be discussed in the next section.

B. Phonon Structure

BCS theory describes the superconducting state for electron energies close to the Fermi surface. However in regions of higher energies the theory is not entirely in accord with experiment. This indicates that the simplifying BCS assumption of a cut off for both Coulomb and phonon interaction at $\hbar\omega_q$ requires modification. Bardeen (1959) has pointed out that the cut off may be determined by the lifetime of the quasi-particles that can be excited across the gap. The effect of this on the pair interaction has been discussed by Eliashberg (1960), who succeeded in extending Bogoliubov theory to include both lifetime effects for the excited electrons and an explicit phonon distribution. Green's function techniques have been used to account for lifetime effects. It has been found that the energy gap parameter Δ is a complex function of energy. Swihart (1962) and Morel and Anderson (1962) assumed a model in which the interaction V is energy dependent. They showed that lifetime effects are too small to justify cutting off the Coulomb repulsion at $\hbar\omega_{\vec{q}}$. Therefore they include in the interaction a repulsive part ($V > 0$) for energies $\varepsilon_k > \hbar\omega_q$. The resulting variation of the energy gap at 0°K as a function

of ε_k has been shown by Morel and Anderson to have the form represented in fig. (3-2).

Equation (2-24) indicates that any variation in the energy gap should be reflected in a variation in the density of states. Since the current in the tunneling experiment is proportional to the density of states, we may obtain the relative change in the density of states directly by plotting the relative conductance σ versus the applied voltage V. Giaever, Hart and Megerle (1962) found good agreement between the data and BCS theory for Sn, In and Aℓ. However for Pb, definite divergences exist from the BCS density of states. Adler and Rogers (1963) observed similar divergences in the case of In. Corresponding to these divergences in the relative conductances versus energy curves, there are bumps in the I-V characteristics. It has been suggested that these variations may be accounted for by using a variable energy gap parameter $\Delta(\varepsilon)$ which changes sign at $\varepsilon \simeq K_B\theta_D$.

Schrieffer, Scalapino and Wilkins (1963), have used the tunneling formalism to investigate the structure in the density of superconducting states due to a model phonon spectrum for Pb. Two Lorentzian distributions whose parameters are chosen to fit the neutron scattering data for Pb are shown in fig. (3-3). They also found that the possibility of transferring electrons from one film to the other results in a complex energy gap parameter, and that the reduced density of states is given by

$$\rho_T(E) = R.P. \frac{E}{(E^2 - \Delta^2)^{\frac{1}{2}}} ,$$

where $\Delta = \Delta_1 + i\,\Delta_2$. Using a binomial expansion valid for $\Delta/E << 1$

Fig. (3-2) The energy gap at 0°K as a function of energy ε_k as shown by Morel and Anderson (1962).

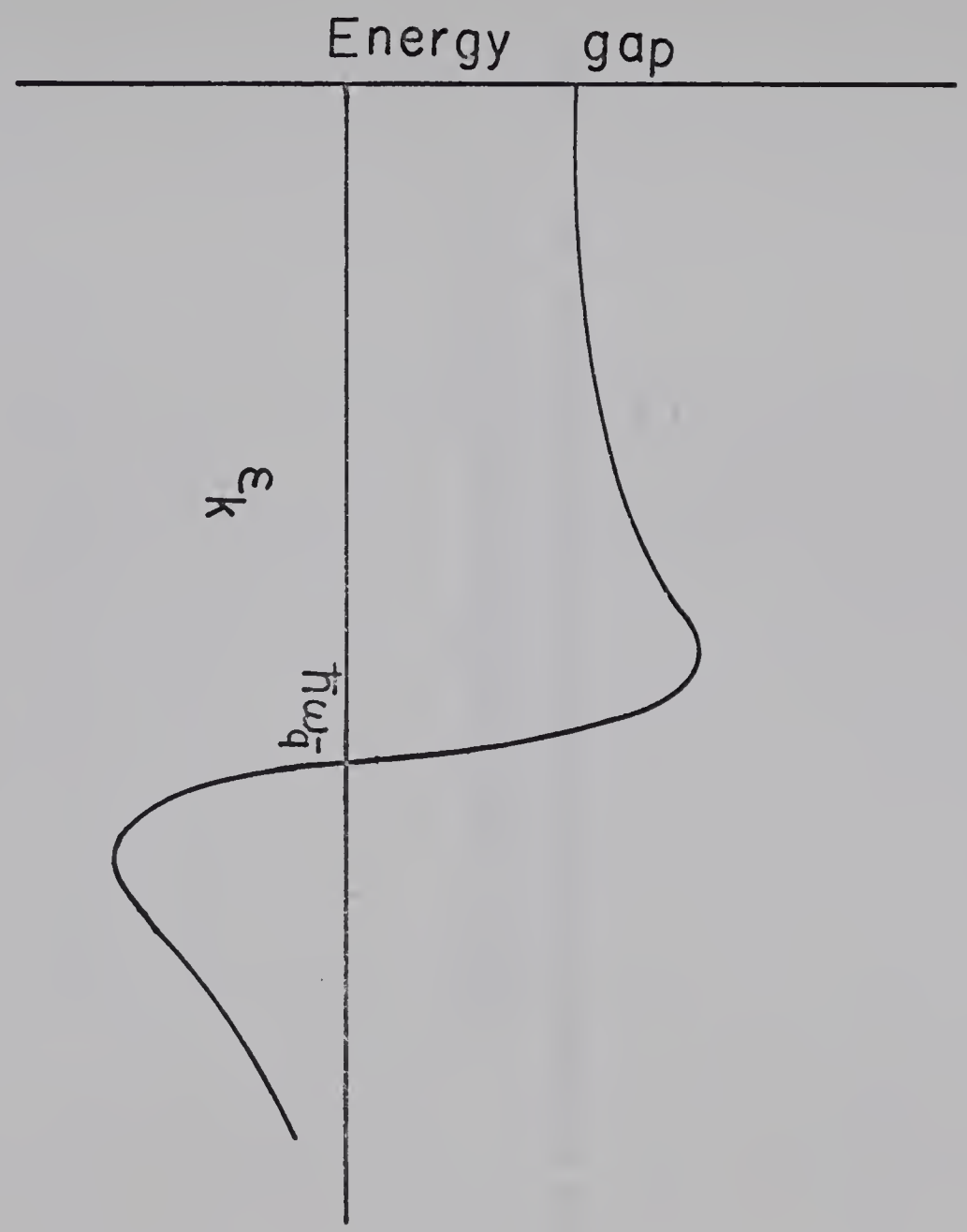
Energy gap
k_3
$\hbar\omega_q$

Fig. (3-3) The two Lorentzian distributions whose parameters are chosen to fit the neutron scattering data for Pb.

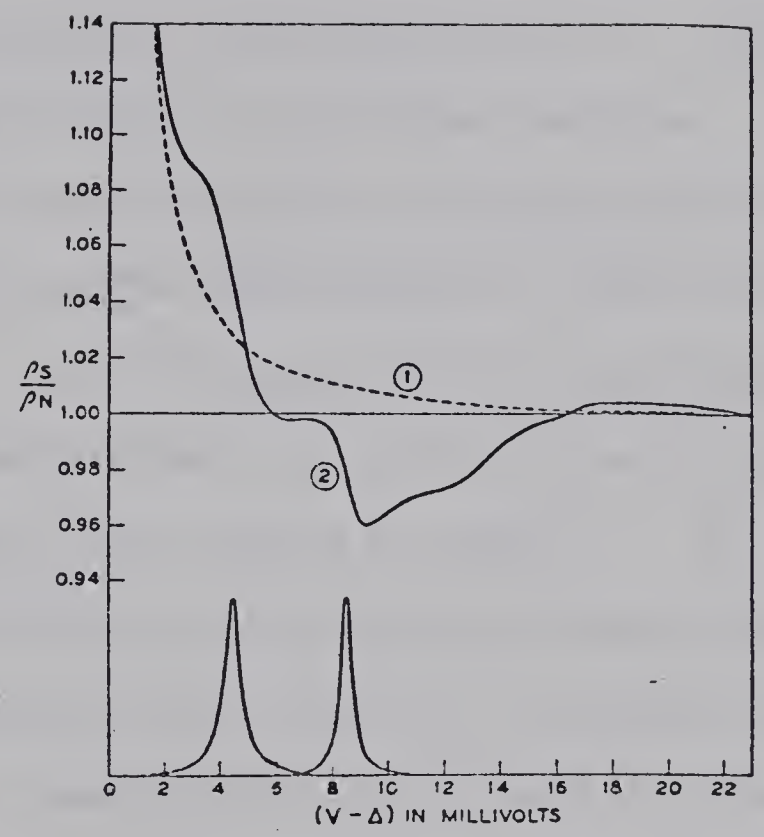

The variation with energy of the ratio of density of states in superconducting lead to that in the normal metal. Curve 1 is the BCS plot, curve 2 the tunneling measurement. Also shown is the phonon spectrum suggested by the experimental density-of-states plot.

we find

$$\rho_T(E) = 1 + \frac{1}{2E} (\Delta_1^2 - \Delta_2^2) \quad .$$

So in an energy region where Δ_2 is larger than Δ_1, the tunneling density of states falls below that of the BCS theory.

Rowell et al (1963) looked for the sharp peaks in d^2I/dV^2 that occur at voltages corresponding to inflections in dI/dV. These peaks are related to the Van Hove singularities of the phonon spectrum.

Van Hove (1953) proved that for a three dimensional crystal, there exist in the phonon spectrum ($g(\omega)$) versus ω at least two infinite discontinuities in $dg/d\omega$, and at the upper end of the spectrum $dg/d\omega = -\infty$. These infinite discontinuities occur at the values of $\omega(q_c)$ for which the critical points q_c's are defined by $d\omega/dq|_{q_c} = 0$. The effect of the critical points on the second derivative versus voltage plot of N-S and S-S junctions has been considered by Scalapino and Anderson. Their result is that superimposed on the density of states, is a variation that is attributed to the general shape of the phonon spectrum, with singularities of the type represented in table(3.1).

Earlier Morel and Anderson had pointed out that an Einstein phonon peak at energy E_E will produce structure in the density of states at energies

$$\Delta + nE_E \quad , \quad (n = 1, 2, ...)$$

These types of singularities are well discussed by Rogers (1964) for Pb, Sn and In samples.

Table (3.1)

Junction	dg/dv	d^2I/dv^2	Energy of the critical point
N-S	∞	logarithmic singularity and jump discontinuity	$\Delta + E_c$
S-S	∞	logarithmic singularities	$2\Delta + E_c$
	finite		

CHAPTER 4

EXPERIMENTAL TECHNIQUES

A. Sample Preparations

A tunnel junction consists of an evaporated base layer of one metal, a layer of oxide of this metal, and an evaporated metallic cover layer. The films are deposited onto a glass substrate. Tunnel junction preparation with a base layer of Aluminum is described in detail by Adler, Rogers, Khanna and Penner. The critical step in the preparation of a specimen is the oxidation of the base layer to produce a barrier layer with specified characteristics. Aluminum oxide can be formed even in air at room temperature. At elevated temperatures and in the presence of water vapour, the rate of growth of the Aluminum oxide layer is much faster. It is found that the resistance of tunnel junctions is a function of time, temperature, and the metal deposited for the cover layer. At room temperature, the junction resistance increases very rapidly immediately after its preparation and slower after that. At liquid air temperature, the resistance is almost constant with time.

The junctions used in this work are:

$$Sn - SnO - Sn \quad , \quad Sn - SnO - Pb \quad , \text{ and } \quad Pb - PbO - Pb \quad .$$

They have different behaviour and require a slightly different method of preparation. A special cell, shown in fig. (4-1), is used. It was constructed for the purpose of preparing double tunnel junctions like

Fig. (4-1) The cell which is used for tunnel junctions preparation.

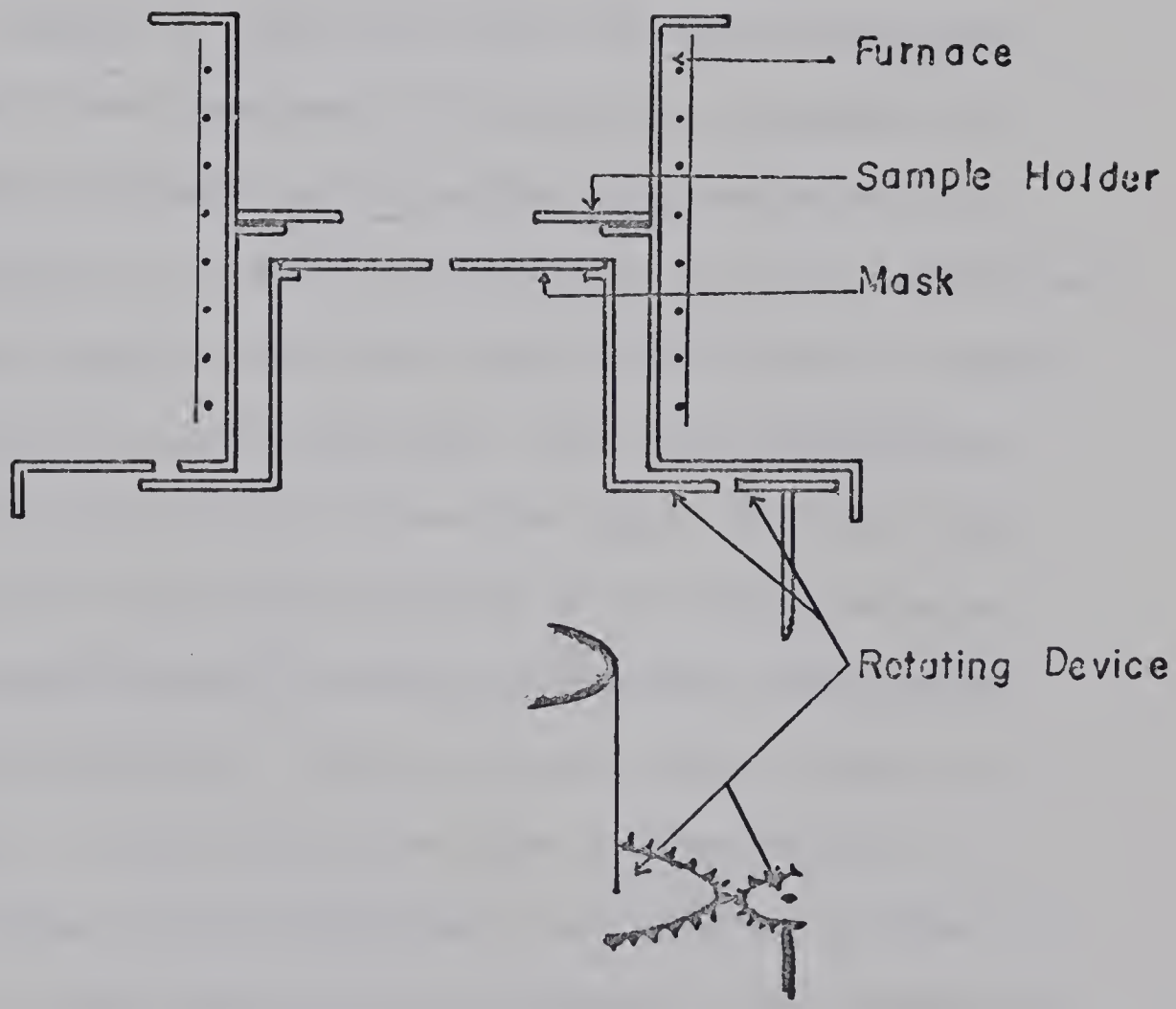
Furnace
Sample Holder
Mask
Rotating Device

Pb - PbO - Pb - PbO - Pb. The cell is provided with a sample holder situated just behind a rotating mask which is mounted in the middle of a furnace. The mask is a separate part, that can be easily removed for cleaning or replacement. The furnace temperature ranges from 20°C to 300°C. It was possible to control some parameters, like humidity and oxygen pressure, which might affect the formation of the oxide layer.

The glass substrates used are pieces of clean microscope slide one inch square. Indium is smeared at the positions of the prospective electrical leads. Usually the leads are indium soldered to the films after the tunnel junction is completed, but for the tin junctions, it was necessary to smear the indium solder on the substrate before any film deposition because the tin films are destroyed by contact with molten indium. It was found that the tin-indium contact often showed a tunnel junction characteristic at room temperature. This could sometimes be destroyed by applying a high voltage across the leads connected to the film. The formation of these tunnel junctions is not likely to occur if the indium is slightly scraped to remove any possible indium oxide just before the film deposition. The substrate with indium smears is shown in fig. (4-2a). A fairly thick base layer is evaporated in (10^{-6} Torr.) vacuum from a heated molybdenum boat carrying a charge of 99.999% pure tin. Measurements of the resistances of such films show that they are approximately 500 $\mathring{A}$ thick. The base layer is shown in fig. (4-2b).

Two methods of oxidation were tried; the glow discharge method described by Miles and Smith (1963), and a thermal oxidation method.

Barriers obtained by the first of these methods were very poor. Metallic bridges were likely to exist through the oxide layer. The current-voltage characteristic of one of these junctions displayed on the screen of an oscilloscope is shown in fig. (4-3). Notice that, for small voltages, the current increases with the applied voltage, after which many discontinuities occur in the I-V characteristic. These have been reported by Giaever (1961) and observed by Rogers (1964). The thermal oxidation method was used to prepare all the tunnel junctions investigated in this work. The base layer is allowed to oxidize for two or three hours at nearly 75°C in dry oxygen at atmospheric pressure. The oxygen is dried by passing it slowly over sodium hydroxide and through a coil of copper surrounded by a mixture of dry ice and acetone.

The next step is to evaporate a cover layer of tin or lead to obtain the required tunnel junction. See fig. (4-2c). The evaporation rate of the cover layer was equal or slightly less than that of the base layer to avoid barrier destruction. The evaporation time was long enough to produce a continuous film. Resistance measurements show that the thickness of these layers is approximately 1000 $\mathring{A}$.

About half an hour after a cover layer of tin was deposited, the resistance of the junction was essentially zero. However, the resistance increases with time, in contrast to Aluminum junctions, slowly at the beginning and faster at later times. As soon as it reaches the required resistance, it is mounted and immersed in liquid air. No further change in the junction resistance was observed during periods as long as one week.

The most stable junction is Pb-PbO-Pb. These films are also evaporated

Fig. (4-2) The various steps of the sample preparation.

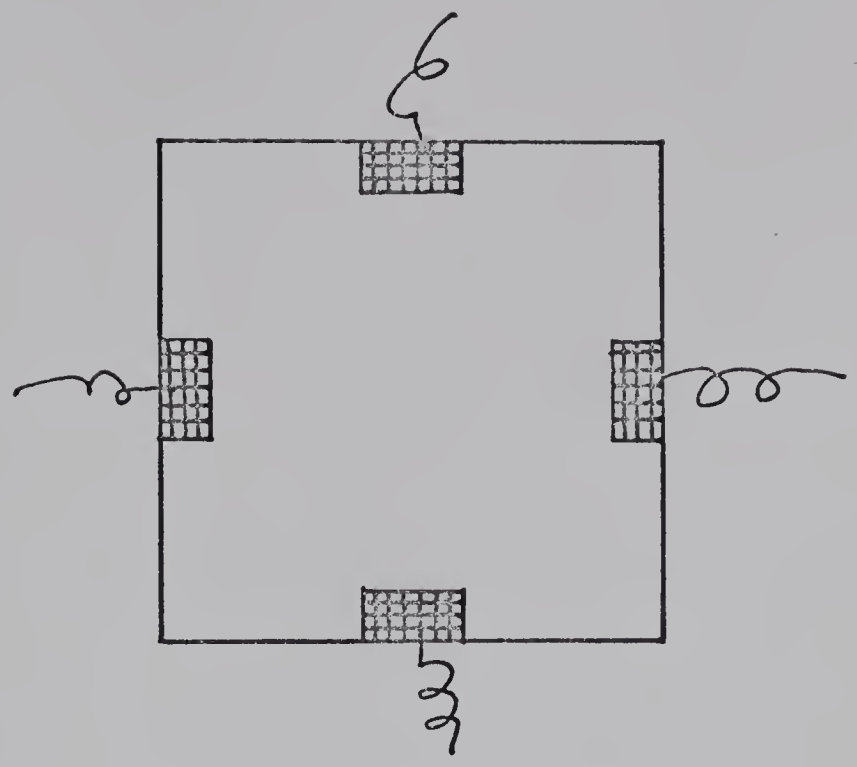

(a)

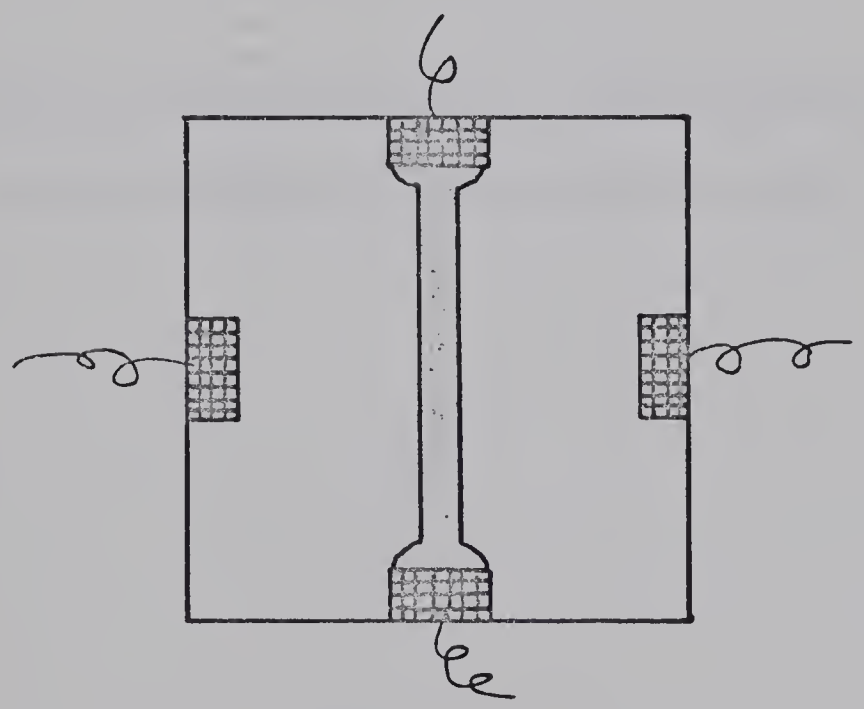

(b)

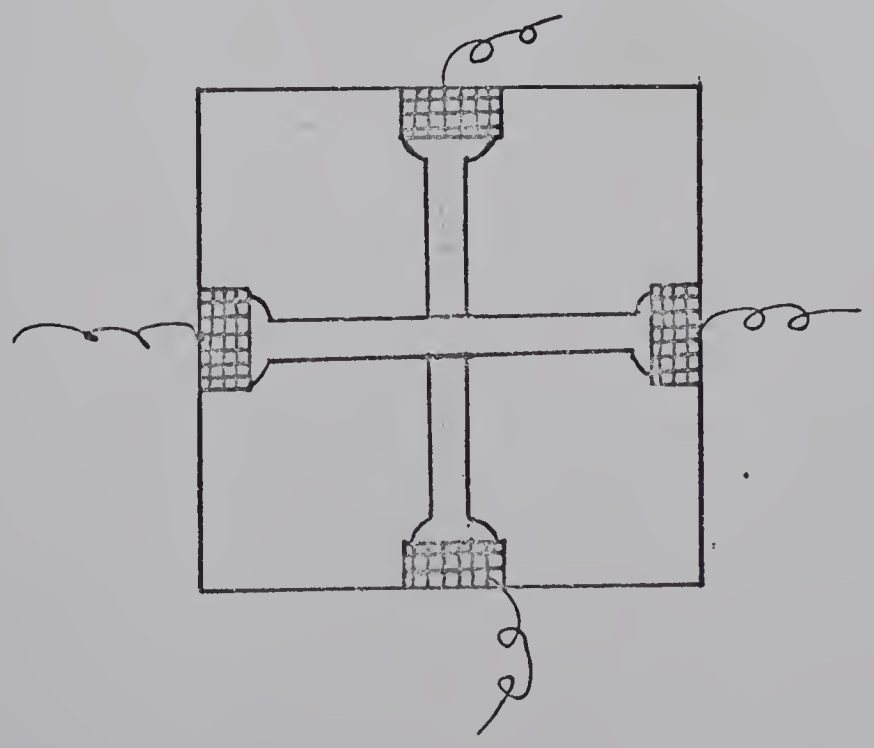

(C)

Fig. (4-3) The I-V characteristic of a Sn-Sn junction which contains metallic bridges through the oxide layer.

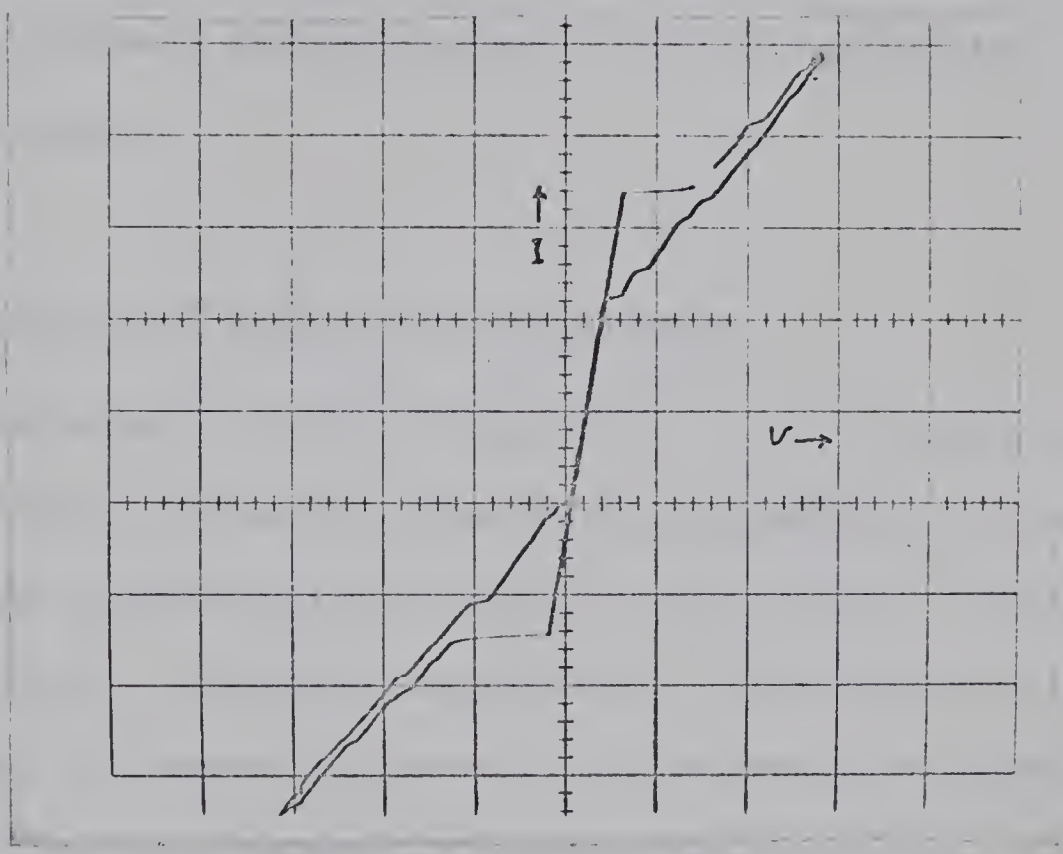
I
V

from a molybdenum boat onto a glass substrate placed very close behind a fairly thick mask to avoid a shadow formation. The evaporated films were made very narrow to decrease the possibility of metallic bridges in the oxide layer. Wider films result in a tunnel junction with almost zero resistance. The base layer was oxidized in the way described above, but the oxide layer formation is very sensitive to water vapour. A zero resistance oxide layer is always obtained if the oxygen contains a small amount of water vapour.

B. Dewar Description and Temperature Measurements

The apparatus which is shown in fig. (4-4) consists basically of a glass dewar for liquid helium with provisions for pumping on the helium, and an outer dewar containing liquid nitrogen which acts as a radiation shield for the helium. A heater, consisting of a 500 Ω carbon resistor and a small piece of copper, is located at the bottom of the internal dewar. Its function is to remove the liquids from that dewar. The inner dewar is provided with a loose plug of styrofoam at the top to reduce the evaporation rate of liquid helium.

Samples are immersed directly in the helium bath; this provides a good thermal coupling between the bath and the sample. Temperatures are determined from measurements of the helium vapour pressure. The pressure is controlled by means of a manostat with a flexible membrane. In such an arrangement, temperature inhomogeneities in the liquid helium may make the recorded vapour pressure a rather poor indication of the temperature at points within the liquid. A stationary temperature can be maintained

Fig. (4-4) The glass dewar for liquid helium.

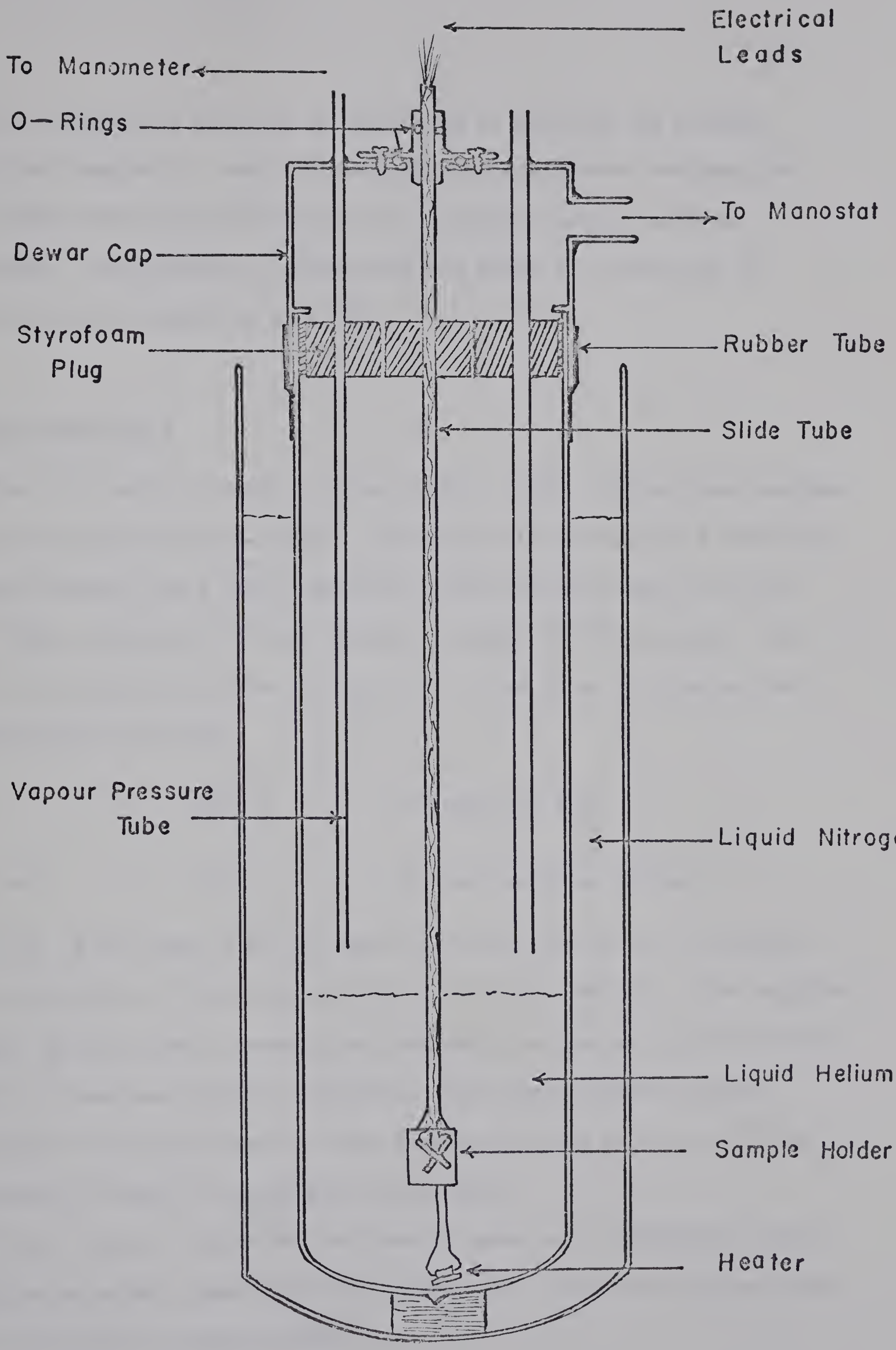
Electrical Leads
To Manometer
O—Rings
To Manostat
Dewar Cap
Styrofoam Plug
Rubber Tube
Slide Tube
Vapour Pressure Tube
Liquid Nitrogen
Liquid Helium
Sample Holder
Heater

if the corresponding pressure is approached by reducing the pressure slowly and regularly. Small corrections to the manometer readings for temperature and g-value differences from standard values have been neglected. The accuracy in temperature was about $\pm$ 0.1 per cent in the temperature range from 2 to 4°K.

C. Instrumentation

The I-V tracing circuit is shown in fig. (4-5). It has been designed and constructed by Rogers (1967). The circuit is provided by a sensitive current-detector and a small impedence current source (nearly vertical load line), in order to detect currents as small as 10^{-7} amperes. The idea of the circuit is shown in fig. (4-6). The point of intersection V satisfies the equations:

$$I = \frac{V_B - V}{R} \qquad \text{for the load line}$$

and $$I = I(V) \qquad \text{for the tunneling current.}$$

The locus of the point V as the load line moves outward with a constant slope yields the I-V characteristics of the tunnel junction. The supplied voltage V_B can be swept smoothly and uniformly in time at a rate which is polarity, range and vernier adjustable. The sweep amplitude control attenuates the output from the sweep generator, shown in fig. (4-7), to a convenient range for energy gap measurements.

The σ versus v traces are obtained by means of a conductance bridge described by Adler, Roger and Woods (1964). The bridge has been modified and is described by Rogers (1967).

Fig. (4-5) The I-V tracing circuit.

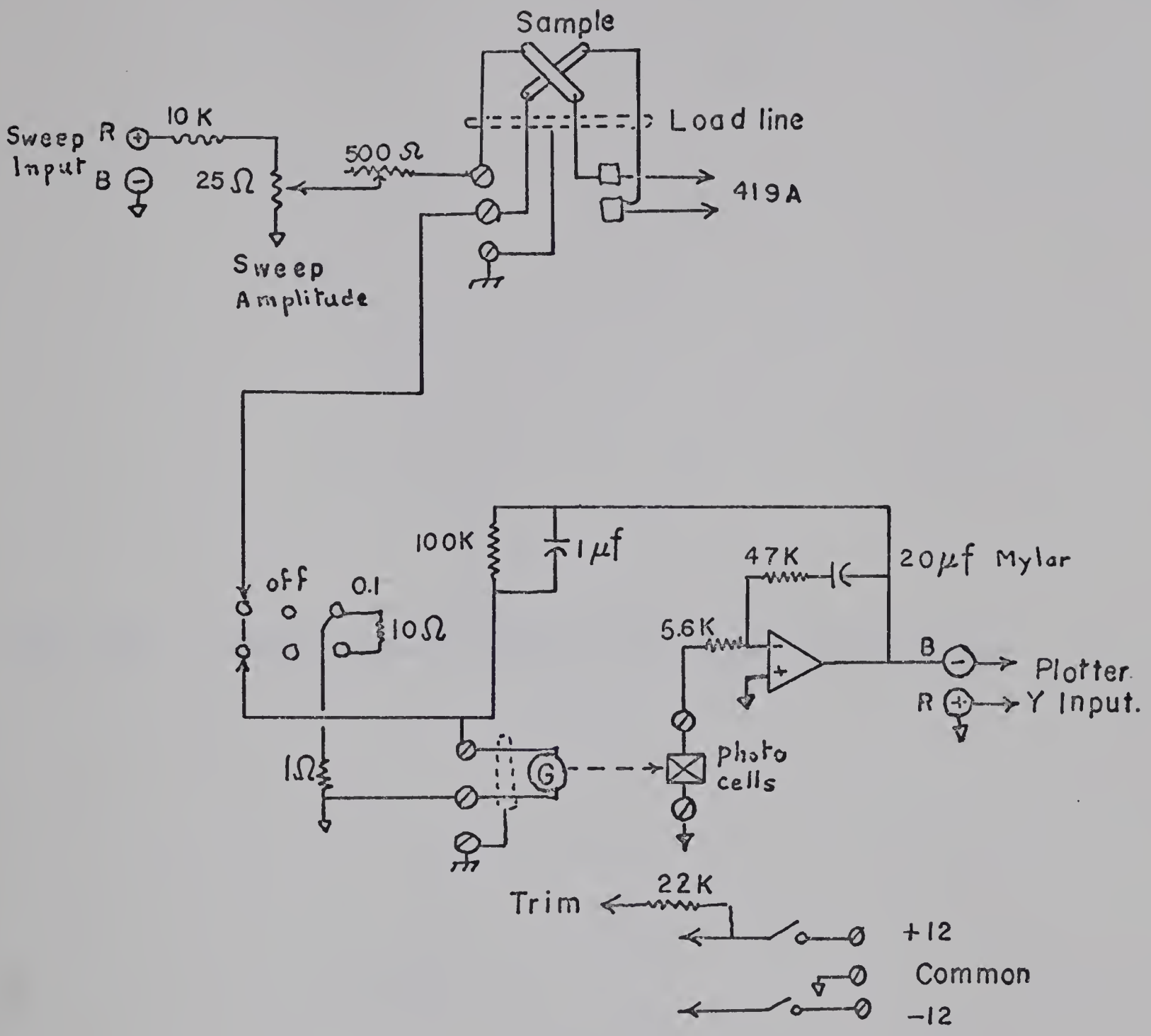
Sample
Load line
10 K
Sweep R
Input B
25 Ω
500 Ω
419 A
Sweep
Amplitude
100K
1 μf
47K
20 μf Mylar
off
0.1
10 Ω
5.6K
B
Plotter
R
Y Input.
1Ω
G
Photo
cells
22K
Trim
+12
Common
-12

Fig. (4-6) Schematic showing the idea of the I-V tracing circuit.

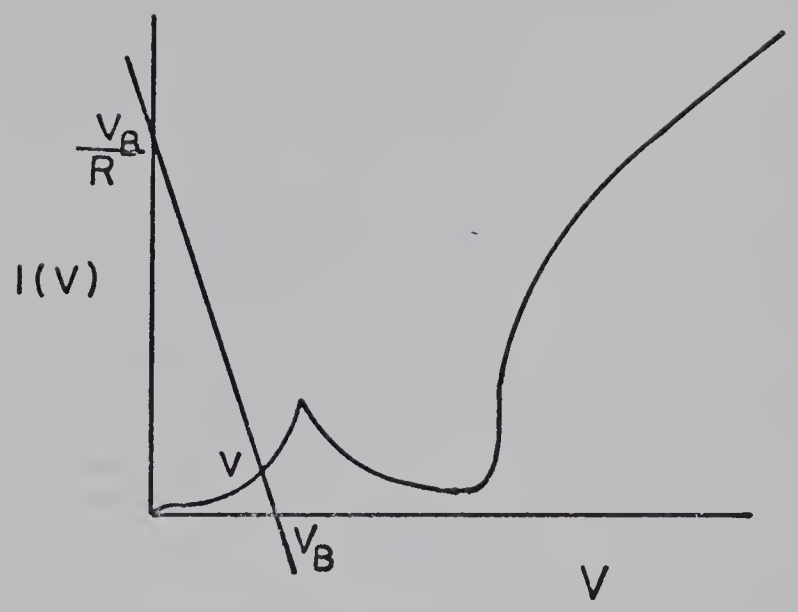

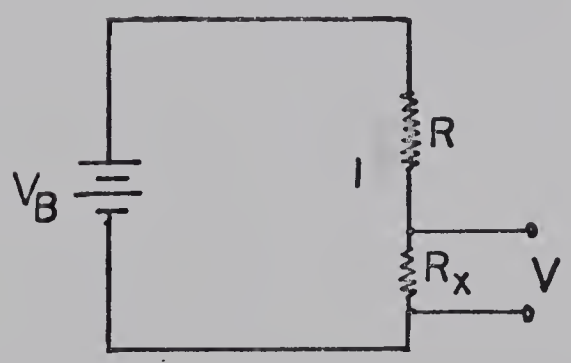

$$I = \frac{V_B - V}{R} \qquad \text{(Load line)}$$

$$I = I(V) \qquad \text{(Junction)}$$

Fig. (4-7) The sweep generating circuit.

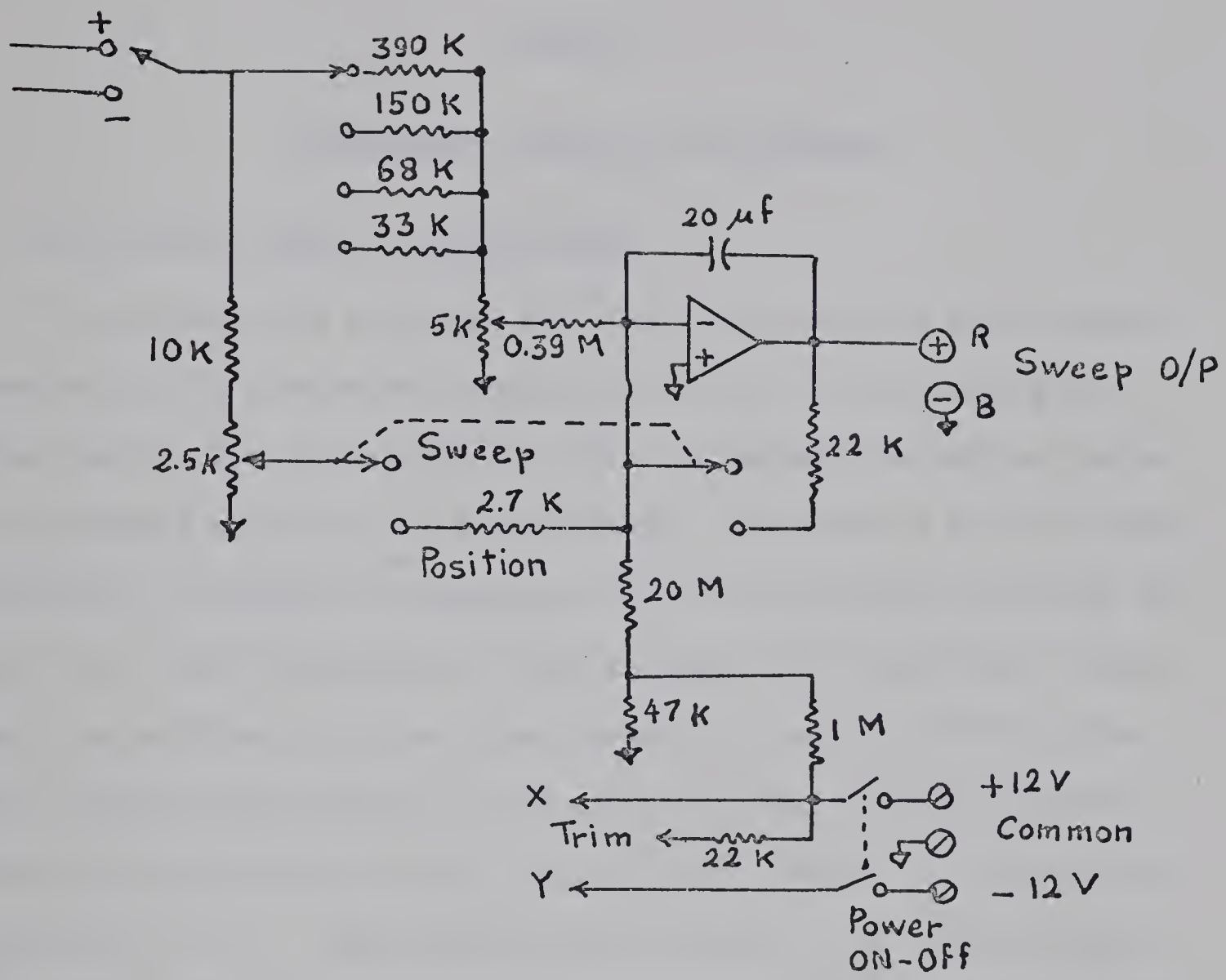
+
−
390 K
150 K
68 K
33 K
20 μf
10 K
5K
0.39 M
R
Sweep O/P
B
2.5K
Sweep
22 K
2.7 K
Position
20 M
47 K
1 M
X
+12 V
Trim
22 K
Common
Y
− 12 V
Power
ON-OFF

CHAPTER 5

EXPERIMENTAL RESULTS AND DISCUSSION

A. The Relative Jump in Specific Heat

Fig. (5-1) shows a typical I-V characteristic for a Sn-Pb tunnel junction at 3°K along with a sample calculation of the energy gaps. (The break in the characteristic within the negative resistance region is attributed to the onset of oscillation). Two sets of the I-V characteristics, at different temperatures, of one of the Sn-Pb junctions and one of the Sn-Sn junctions are shown in figs. (5-2) and (5-3). Notice that the Sn films still show superconductivity even at 3.79°K, while the transition temperature of bulk tin is 3.73°K. A value 3.8°K was chosen for T_c and used to plot $[\Delta_{Sn}(T)/KT_c]^2$ versus $t = T/T_c$ in the range $0.9 \lesssim t \lesssim 1$. These plots are the straight lines shown in figs. (5-4) and (5-5). The actual values of T_c were determined by adjusting the slope of the lines to intersect the t - axis at t = 1. The transition temperatures were 3.81°K for Sn in a Sn-Pb junction and 3.83°K, 3.84°K for Sn-Sn junctions. At these temperatures, a value 1.61 ± 0.02 for the average of the relative jump in specific heat was obtained from the slopes of the lines and equation (2-32).

Tunnel junctions of Sn-Pb with resistances from 0.3 to 4 ohms at liquid nitrogen temperature and thickness in the range from 420 Å to 3670 Å were investigated by Shigi (1968). The transition temperature for Sn in all the samples was found to be 3.86°K, in good agreement with

Fig. (5-1) The typical I-V characteristic of a Sn-Pb junction at 3°K along with a sample calculation of the energy gaps.

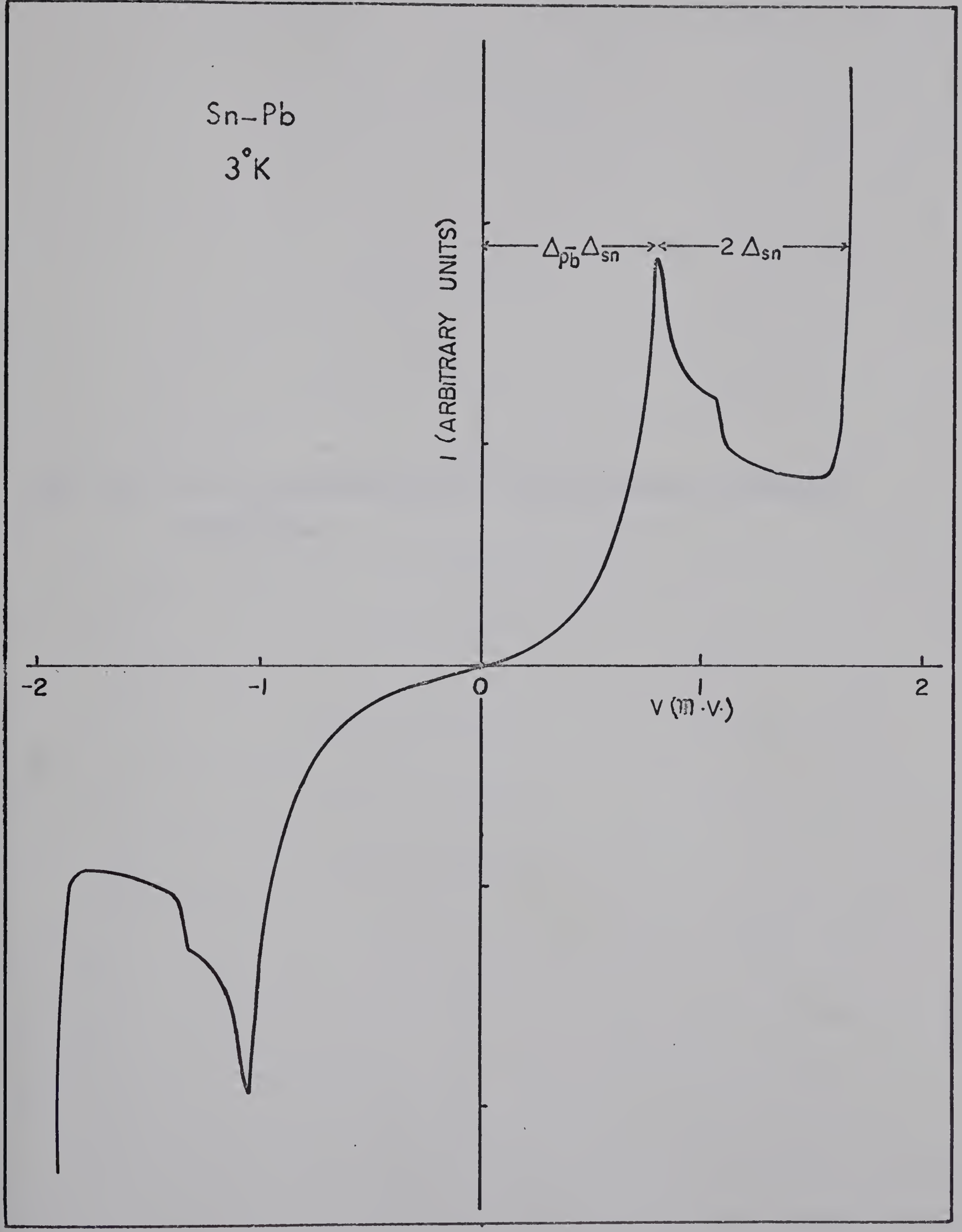
Sn–Pb
3°K
I (ARBITRARY UNITS)
Δ_{Pb} Δ_{Sn}
2 Δ_{Sn}
-2
-1
0
1
2
V (m·V·)

Fig. (5-2) The I-V characteristics of a Sn-Pb junction at different temperatures.

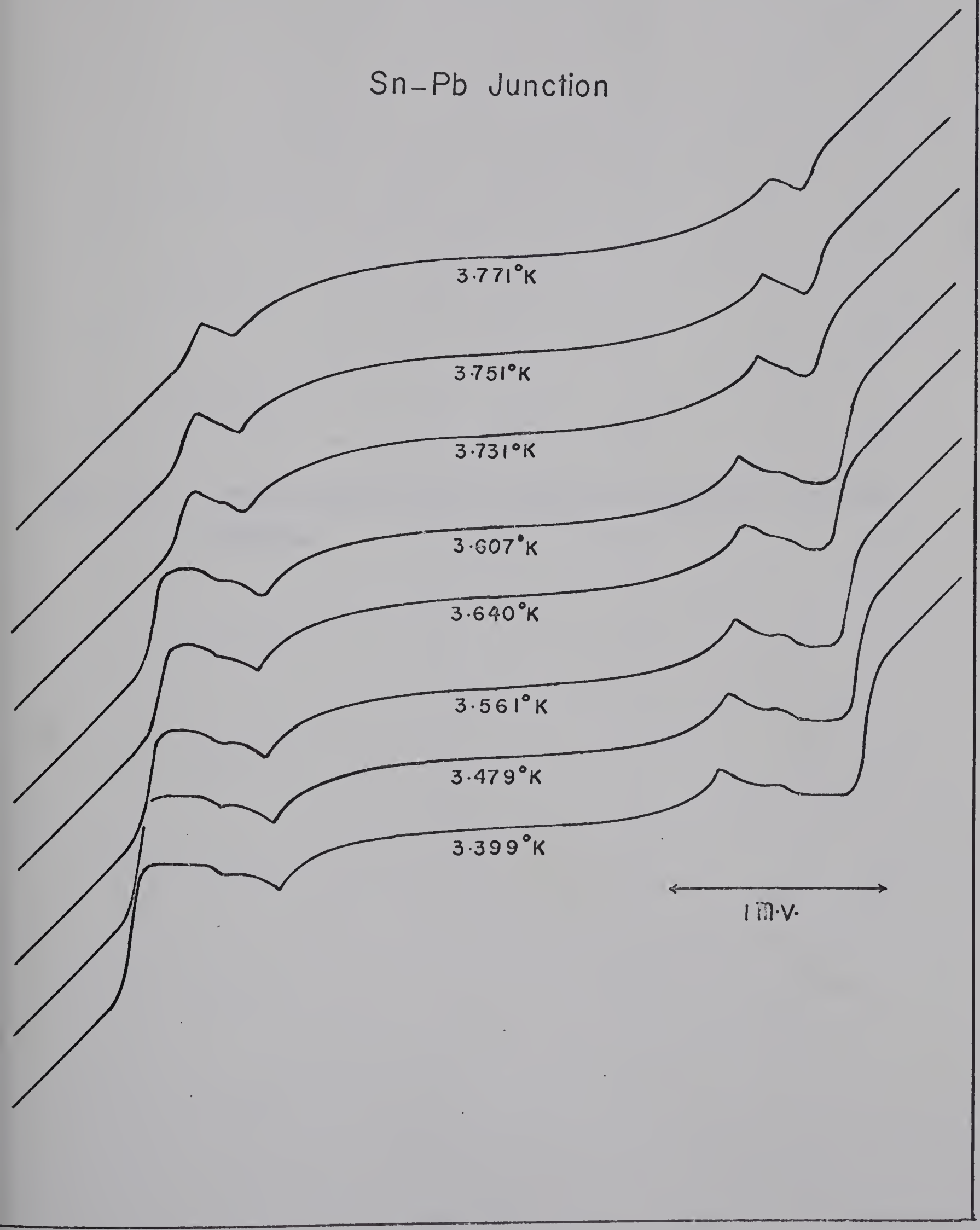
Sn–Pb Junction
3·771°K
3·751°K
3·731°K
3·607°K
3·640°K
3·561°K
3·479°K
3·399°K
1 m·V·

Fig. (5-3) The I-V characteristic at different temperatures of a Sn-Sn junction.


I
0
3·457°K
0
3·424°K
0
3·238°K
0
2·995°K
0
2·704°K
0
2·507°K
0
2·299°K
0
2·081°K
0
1·756°K
0
1
V m·v.

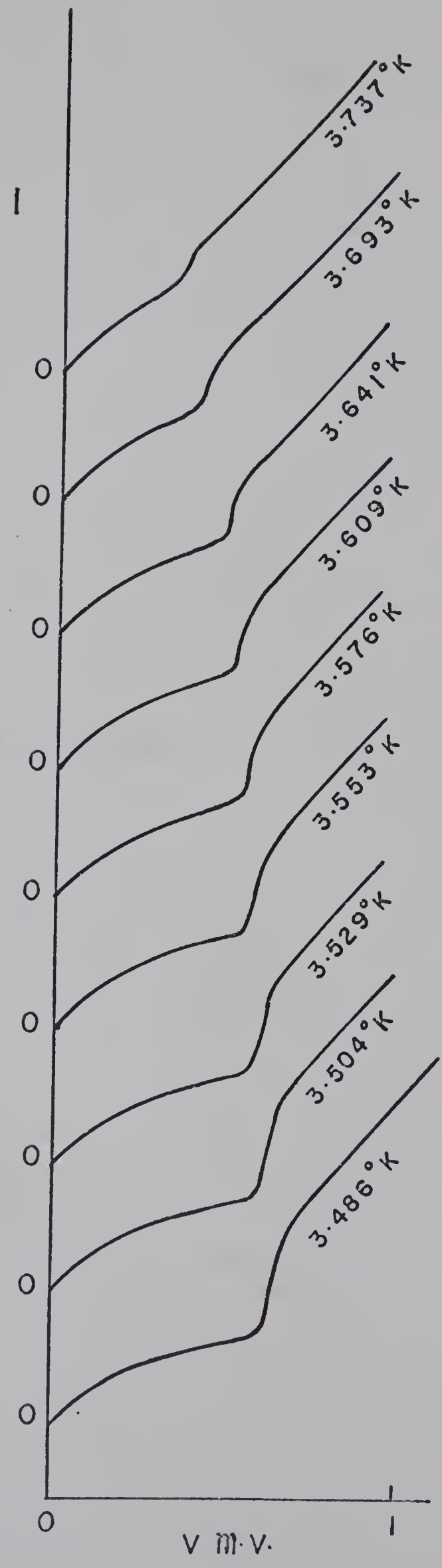
I
0
3·737°K
0
3·693°K
0
3·641°K
0
3·609°K
0
3·576°K
0
3·553°K
0
3·529°K
0
3·504°K
0
3·486°K
0
1
V m·v.

Sn–Sn

Fig. (5-4) $(\Delta/kT_c)^2$ versus $t = T/T_c$ for a Sn-Sn junction.

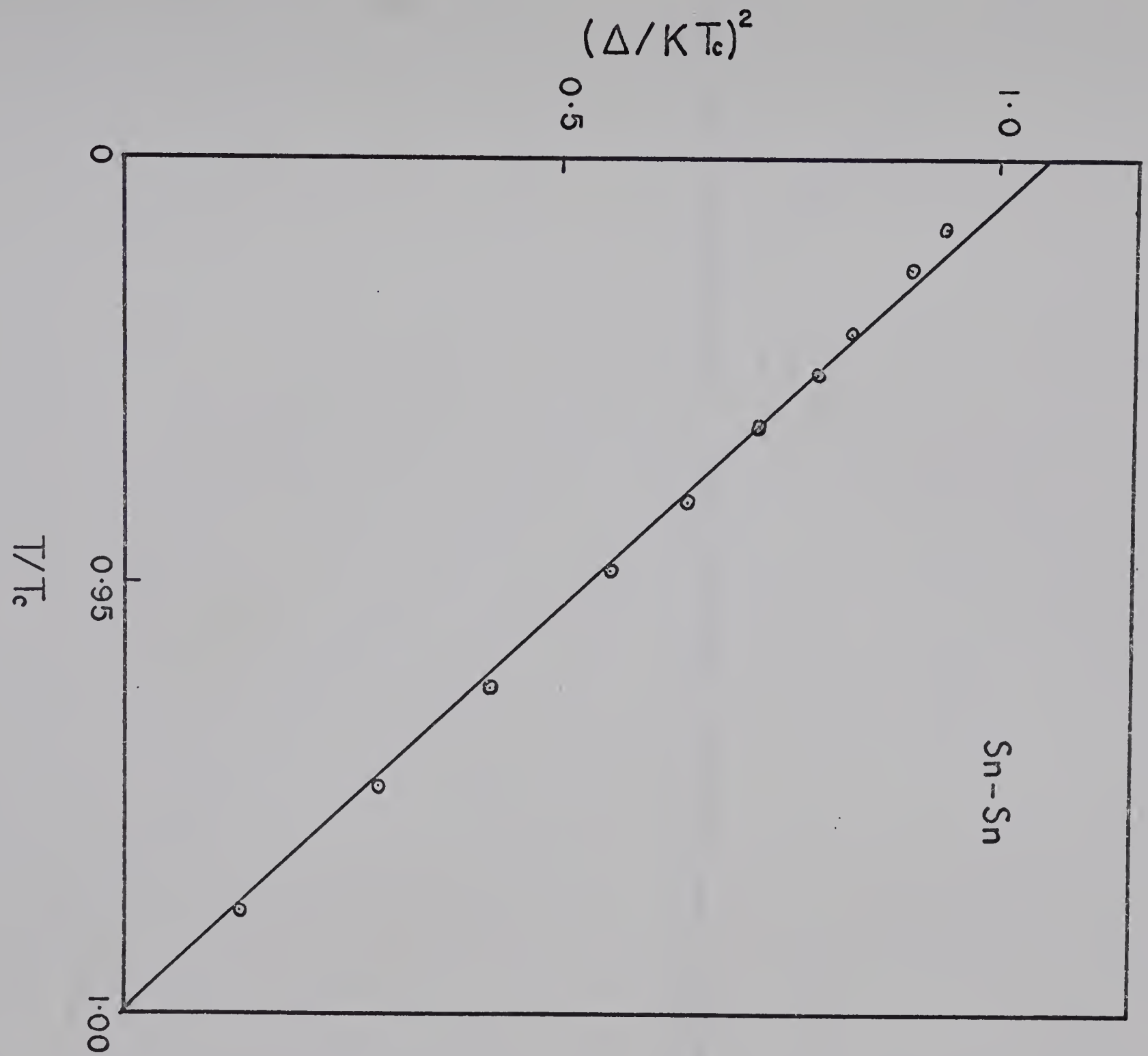
$(\Delta/KT_c)^2$
0
0·5
1·0
T/T_c
0·95
1·00
Sn-Sn

Fig. (5-5) $(\Delta/KT_c)^2$ versus $t = T/T_c$ for Sn-Pb, and Sn-Sn tunnel junctions.

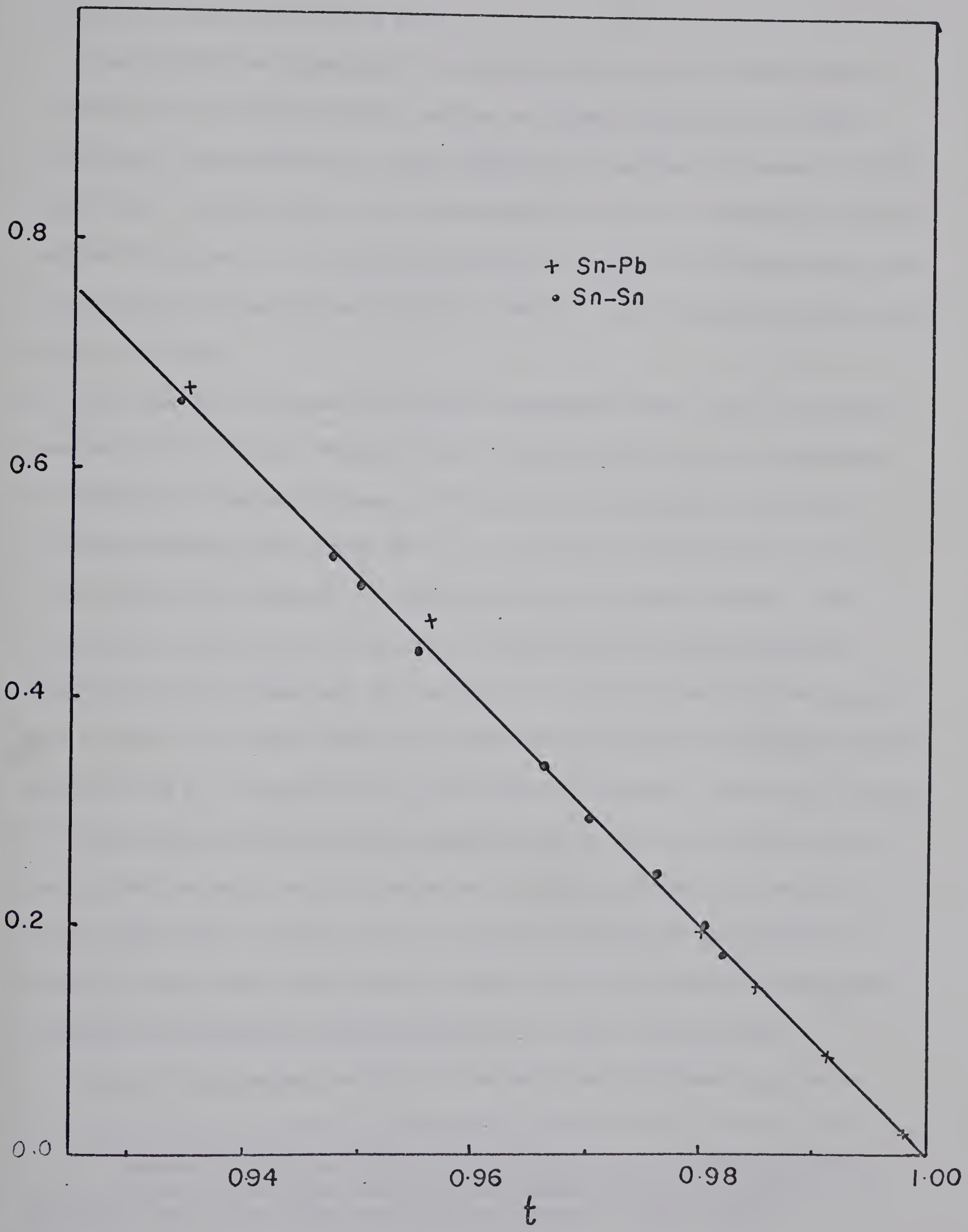
+ Sn-Pb
• Sn-Sn
0.8
0.6
0.4
0.2
0.0
(Δ/KTc)
0·94
0·96
0·98
1·00
t

the values determined in this work.

Lock (1951) has associated the increase in T_c of tin films above the value for the bulk tin with stress in films constrained to follow the thermal contraction of a glass substrate. Jennings and Swenson (1958) showed that a compressive stress decreases the critical temperature while tension increases it. Tin films deposited onto glass substrates were also investigated by Blumberg and Seraphin (1962).* From resistance measurements they found that:

a) The transition temperature varied considerably from sample to sample, even when the thickness and all known control parameters are reproduced. b) There is a regular increase in T_c with decreasing film thickness, for film thickness less than 300 $\mathring{A}$. c) Much of the variation in T_c at the same film thickness is contributed by anisotropy effects. The crystalline orientation of the film is significant in determining the magnitude of the stress and the variation in critical temperature relative to bulk tin. d) The transition width increases with decreasing thickness until for 70 $\mathring{A}$, the width is of the order of 0.070°K. This is in contrast with the result of Walmsley and Campbell (1967), that the current step in the current-voltage characteristics of a tunnel junction is broader in thick films than in thinner ones. In order to minimize the effects of thermal stress, the films should be deposited on substrates whose thermal expansion coefficients closely match those of the film material.

Accurate determination of the electronic specific heat C_{es} can be

---

* Rogers claimed that the transition temperature determined from the resistance of the film itself is unreliable due to edge effect. In Blumberg's work, the films are ruled to remove the edge effects.

made from calorimetric measurements only on those superconductors for which C_{es} is a large fraction of the total specific heat. These measurements provide a test of the assumption that the lattice contribution to the specific heat is the same in both superconducting and normal phases. At very low temperatures, this is in conflict with the experimental results for some superconductors. Brayant and Keesom (1960) found that C_s is less than $C_{\ell n}$ below 0.8°K for Indium. As a consequence of this behaviour, they concluded that it is not possible to estimate C_{es} directly from specific heat data. The electronic specific heat as a function of temperature at very low temperatures can not be obtained from energy gap measurements, since the gap is almost constant over the range $0 \lesssim t \lesssim 0.4$. However, close to the transition temperature, the energy gap is strongly temperature dependent. This provides a measure of the jump in C_{es} at T_c.

This is the first determination of the relative jump in C_{es} for Sn by measuring the energy gap from the I-V tunneling characteristics. The results are in good agreement with the value 1.6 obtained from calorimetric measurements. The magnitude of this jump depends upon the strength of the attractive interaction, the phonon spectrum, and the band structure of the superconductor. In Pb which is strong coupling and which has a less anisotropic Fermi surface and phonon spectrum than Sn, the magnitude of the jump is 2.65 from calorimetric measurements and 2.15 from tunneling measurements (Frank and Keeler 1968).

B. The Energy Gap $2\Delta(T)$ and the Ratio $2\Delta(0)/KT_c$

The ratio $\Delta(T)/\Delta(0)$ as a function of the reduced temperature t along

with the BCS curve is shown in fig. (5-6). For this figure, the value of $2\Delta(0)$ has been adjusted to give a good visual fit with the BCS curve represented by the solid line. From this chosen value of $2\Delta(0) \simeq 1.22$ mv, one obtains a ratio 3.68 for the energy gap $2\Delta(0)/KT_c$. The gap $2\Delta(T)$ also extrapolates to 1.22 mv at 0°K. In table (5-1) the values of T_c and $2\Delta(0)/KT_c$ determined in this work are shown together with some other results.

The temperature dependence of the energy gap, from ultrasonic attenuation experiments, is shown in fig. (5-7) after Morse (1957). In fig. (5-8) we plot the deviations of the results of the electron tunneling experiment and the ultrasonic attenuation experiment, from that of the BCS theory in terms of the reduced temperature t. The average deviation <dt> of the ultrasonic attenuation data from the BCS theory is - 5% for $0.3 < t_{BCS} \lesssim 0.7$ and + 5% for $0.7 \leq t_{BCS} \lesssim 1$, while the electron tunneling points deviation is - 1% for $0.4 \leq t_{BCS} \lesssim 0.6$ and + 1.5 % for $0.6 \leq t_{BCS} \lesssim 1$.

As mentioned in chapter (2), the ultrasonic attenuation experiment requires $\Delta(0) = BKT_c$ instead of the BCS expression, where B is a function of the crystallographic direction. The values of B in the case of Sn for different orientations are given in table (5.2) below, after Shepelev and Filimonov (1965). Privoroboskii (1963) showed in a theoretical analysis that the minimum energy gap of superconducting tin has not been determined, and that it is not located along one of the principal crystallographic directions. The smallest value 2.7 for B has been determined by Zavaritskii (1963) from electron tunneling measurements, by using a single crystal of Sn on one side of a tunnel junction. Thin evaporated films are polycrystalline.

Fig. (5-6) The temperature dependence of the energy gap.

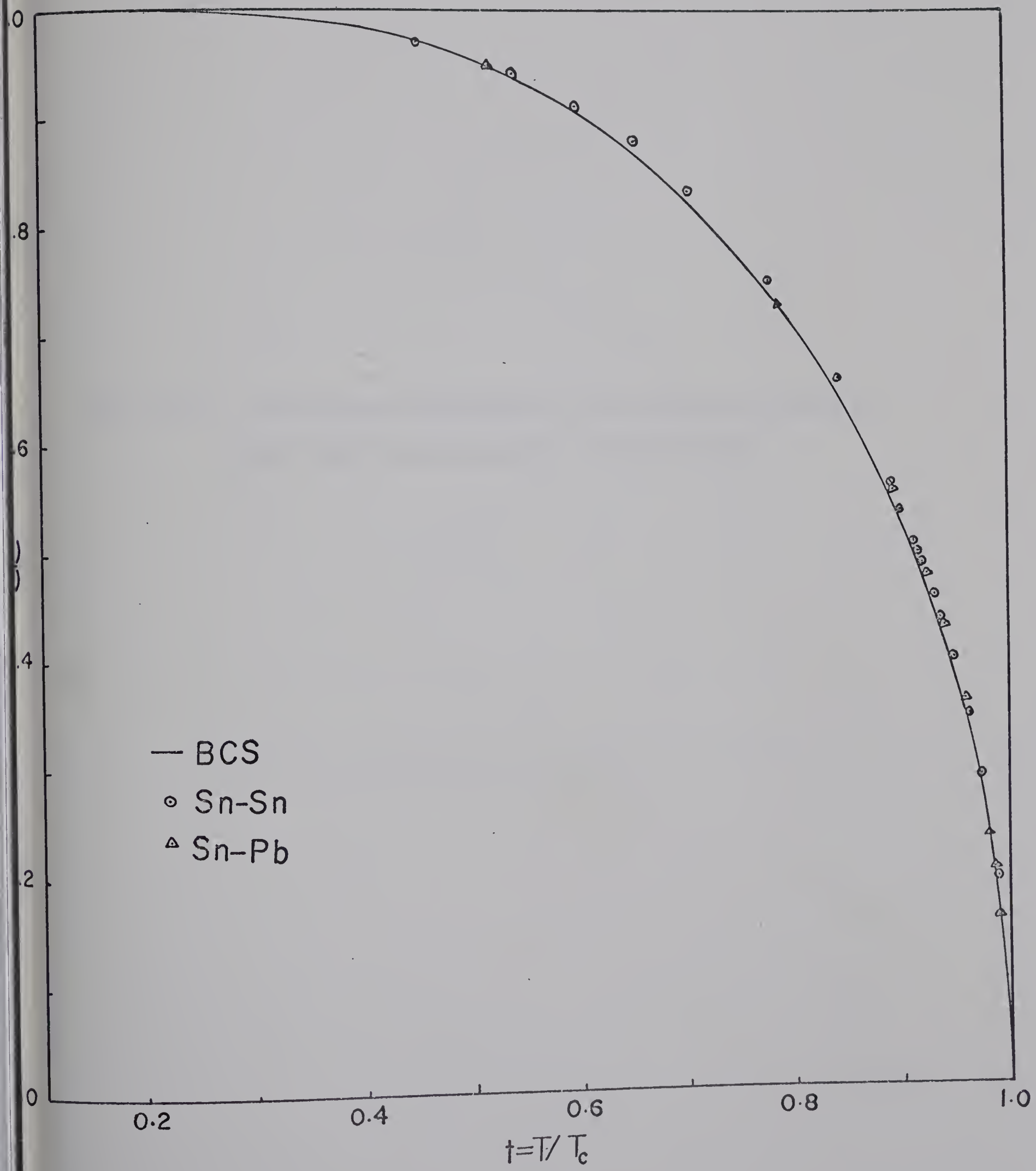
.0
.8
.6
.4
.2
0
0.2
0.4
0.6
0.8
1.0
t=T/ Tc
— BCS
Sn-Sn
Sn-Pb

Fig. (5-7) The temperature dependence of the energy gap obtained by Morse (1957) from ultrasonic attenuation data.

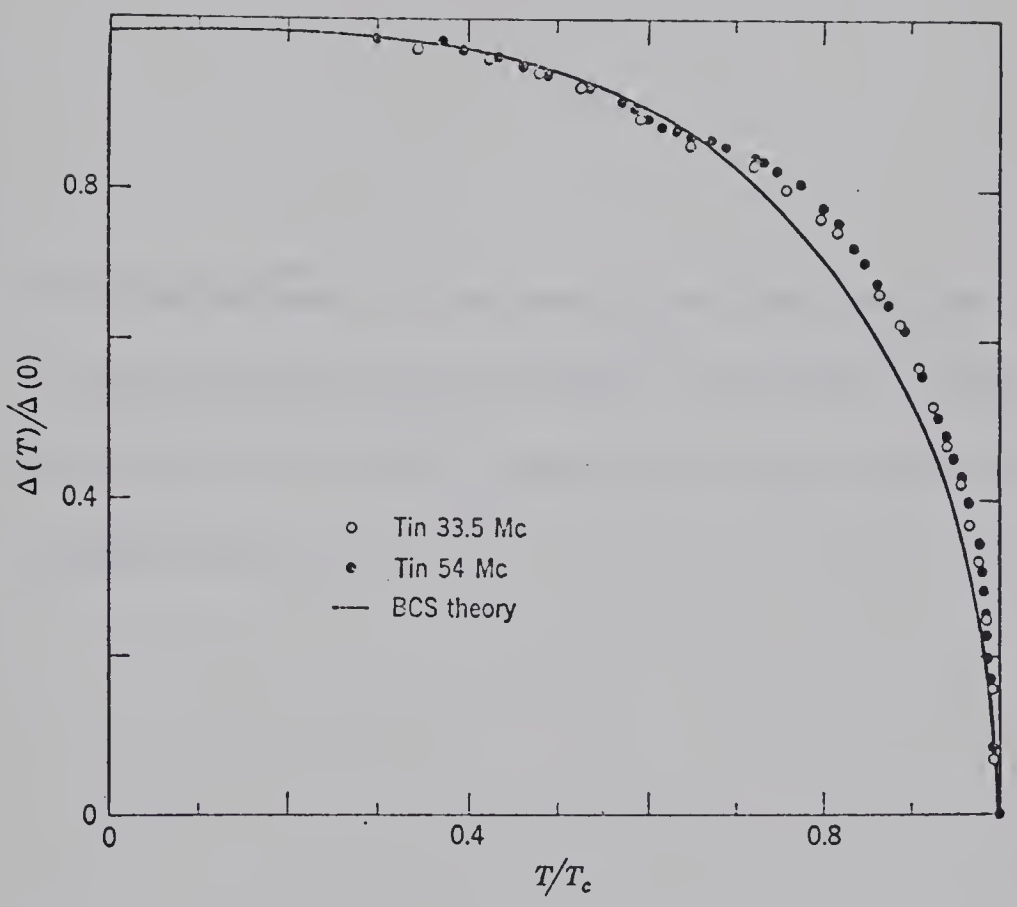

Fig. 5.7 The ratio $\Delta(T)/\Delta(0)$ versus T/T_c. The solid curve is the theoretical result of BCS. The points are the data of Morse and Bohm (M21) from the attenuation of longitudinal sound waves in tin.

Fig. (5-8) The deviations of the results of the electron tunneling experiment and the ultrasonic attenuation experiment from that of the BCS theory in terms of the reduced temperature t.

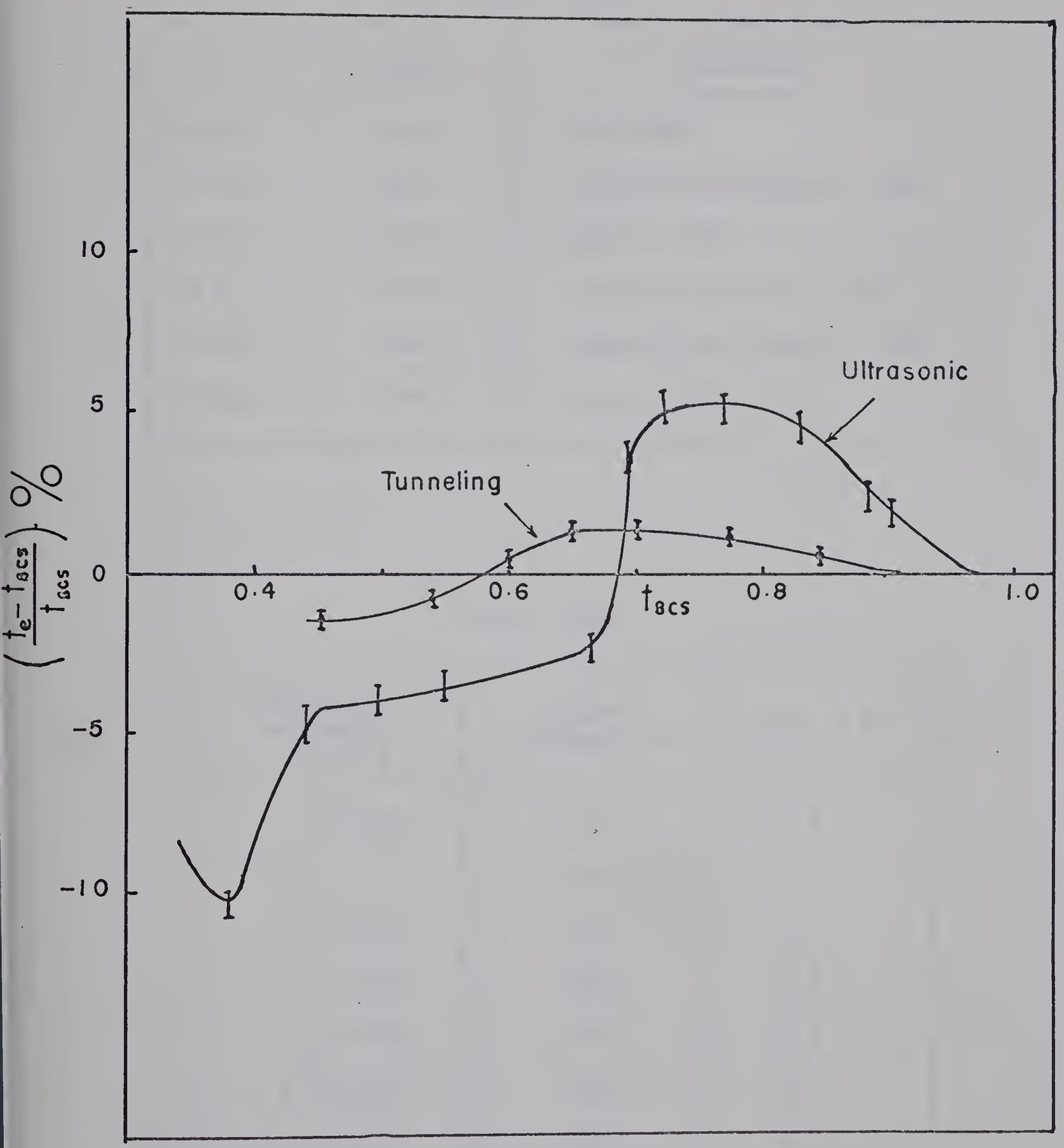
10
5
0
-5
-10
0.4
0.6
0.8
1.0
t_{BCS}
$\left(\frac{t_e - t_{BCS}}{t_{BCS}}\right) \times 100\%$
Ultrasonic
Tunneling

Table (5.1)

T_c	$2\Delta(0)/KT_c$	Reference
3.84	3.68	This work
3.812	3.65	Douglass and Meservey 1964
3.73	3.61	Rogers 1964
3.8	3.51	Townsend and Sutton 1962
3.85	3.67	Walmsley and Campbell 1967
3.86	3.57	Shigi 1968

Table (5.2)

Orientation of accoustic vector k	Maximum frequency MC	$2\Delta_0/KT_c = B$
k $\underline{\mid}$ (101)	257	3.9
K $\underline{\mid}$ (111)	252	4.8
K $\underline{\mid}$ (112)	257	4.4
K $\underline{\mid}$ (211)	276	3.9
K $\underline{\mid}$ (301)	257	4.1
K $\underline{\mid}$ (113)	257	4.0
K $\underline{\mid}$ (311)	215	4.3

For tunnel junctions composed of such films, it is impossible to observe the anisotropy in the energy gap directly. Although the anisotropy is not completely removed, what one can observe is the average of anisotropic energy gaps over the area of the tunnel junction. Such an average may be approximated by assuming that all crystallographic directions contribute equally. The discrepancy in the ratio $\Delta(0)/KT_c$ of film tunnel junctions depends upon which crystalline orientation lies in the plane of the film and which one is perpendicular to it. The crystallographic directions are not reproducible for different films evaporated under conditions which outwardly appear to be the same.

C. Phonon Structure in Sn

The dI/dV versus v characteristic, at a small sensitivity, for a Sn-Sn junction at approximately 2°K is shown in fig. (5-9). In fig. (5-10), the same characteristic is shown at higher sensitivity; the solid line represents the normalized curve, whereas the dashed ones are not normalized. We located the points at which the second derivative d^2I/dV^2 would have maxima and minima. These are represented by the arrows in fig. (5-10). The maxima occur at the critical points 3.3 ± 0.1 mv and 17.6 ± 0.1 mv. The minima occur at 4.5 ± 0.1 mv and 16.1 ± 0.1 mv. There may also be weak structures at 7.9 ± 0.1 mv and 10.8 ± 0.1 mv. The different types of singularities are not analysed here, since the d^2I/dV^2 versus v traces have not been obtained.

The structure in tin is complicated and it was hard to locate the values of energy at which the structure occurs from the first derivative

Fig. (5-9) The dI/dV versus v characteristic of a Sn-Sn junction at 2°K.

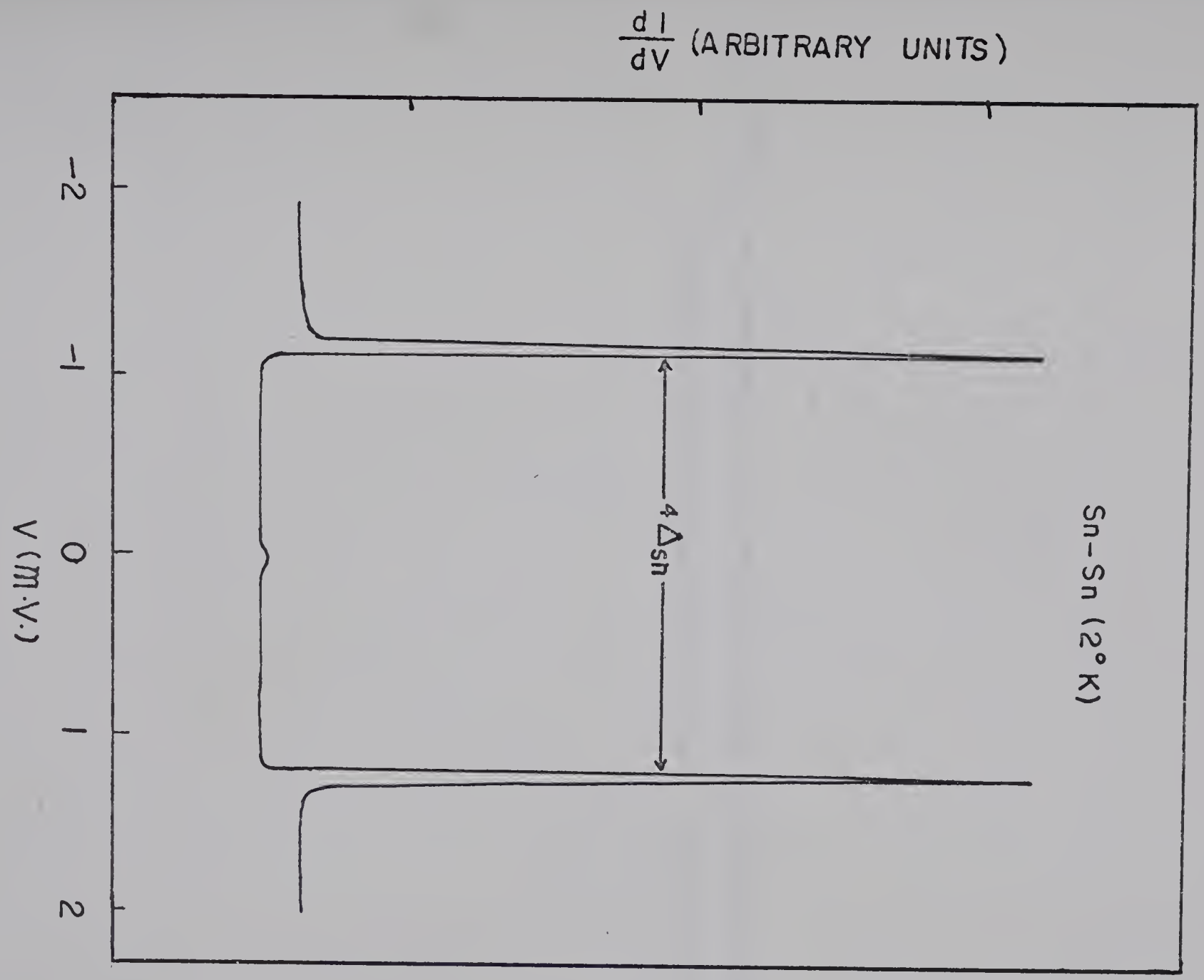
$\frac{dI}{dV}$ (ARBITRARY UNITS)
-2
-1
0
1
2
V (M.V.)
$4\Delta_{Sn}$
Sn-Sn (2° K)

Fig. (5-10) The locations of the critical points at which the phonon structure occurs in the dI/dV versus v characteristic.

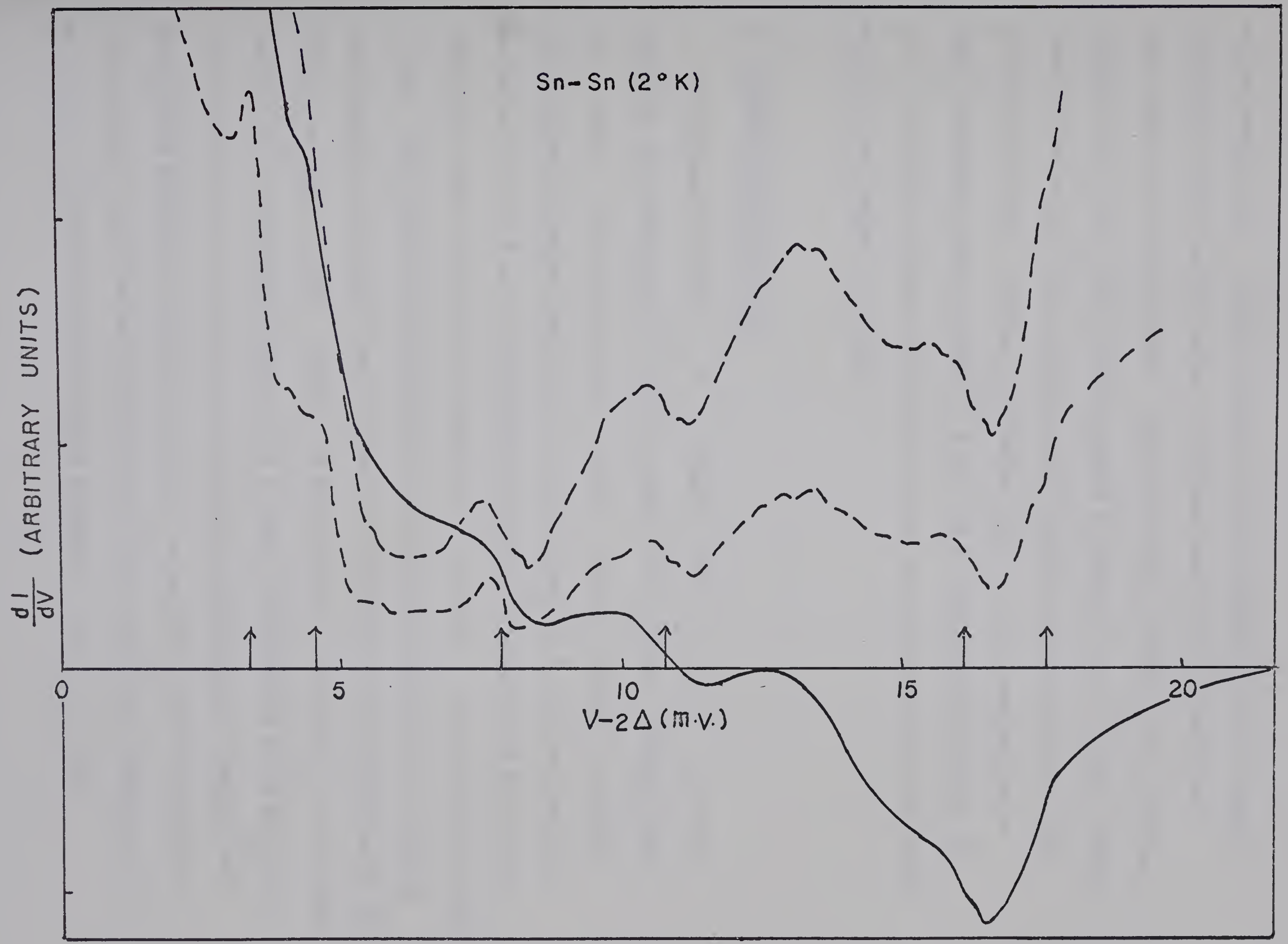
Sn-Sn (2°K)
$\frac{dI}{dV}$ (ARBITRARY UNITS)
0
5
10
15
20
V-2Δ (m.v.)

versus energy plot. Clearer analysis can be obtained from the second derivative versus energy curves. This has been done by Rowell and Kopf (1965) on Sn-Sn junctions. They found that the tin phonon spectrum extends to 17.7 mv, with critical points as low as 3.4 mv. Rogers (1964) observations using Al-Sn junctions, are in good agreement with the work of Rowell and Kopf. He observed further that the tin spectrum has a broad transverse group at about 4.5 mv, and a longitudinal group at 16 mv. The results obtained from this work are in good agreement with Rowell and Kopf, and Roger's results.

D. Phonon Structure in Pb

The phonon structure in Pb is simpler than that of Sn. In a Pb-Pb junction, the energy gap at 4.2°K is found to be 2.56 mv, obtained from the σ versus v trace shown in fig. (5-11). In fig. (5-12a), we observe two transverse groups; the first is located around 3.7 $\pm$ 0.1 mv, and the second at 4.5 $\pm$ 0.1 mv. A longitudinal group is observed at 8.5 $\pm$ 0.1 mv, while some other structures are found at 1.7 $\pm$ 0.1 mv, 3.1 $\pm$ 0.1 mv and 9.0 $\pm$ 0.1 mv. The signs and the location of the critical points are in a fairly good agreement with Rowell and Kopf results (1965) and with Brockhouse *et al* (1962) and Rogers (1964). Rowell and Kopf observed structures at 1.75, 3.05 and 9.0 mv, a transverse group at 4.4 mv and a longitudinal group at 8.5 mv. The structure at 9.0 mv was also observed by Brockhouse as a longitudinal group along different crystal directions. We believe that the structure at 9.0 mv is the second harmonic of that at 4.5 mv, and the one observed at 17 mv in fig. (5-12b) is also the second harmonic of that at 8.5 mv.

Fig. (5-11) The energy gap in Pb calculated from the dI/dV versus v characteristics of a Pb-Pb junction.

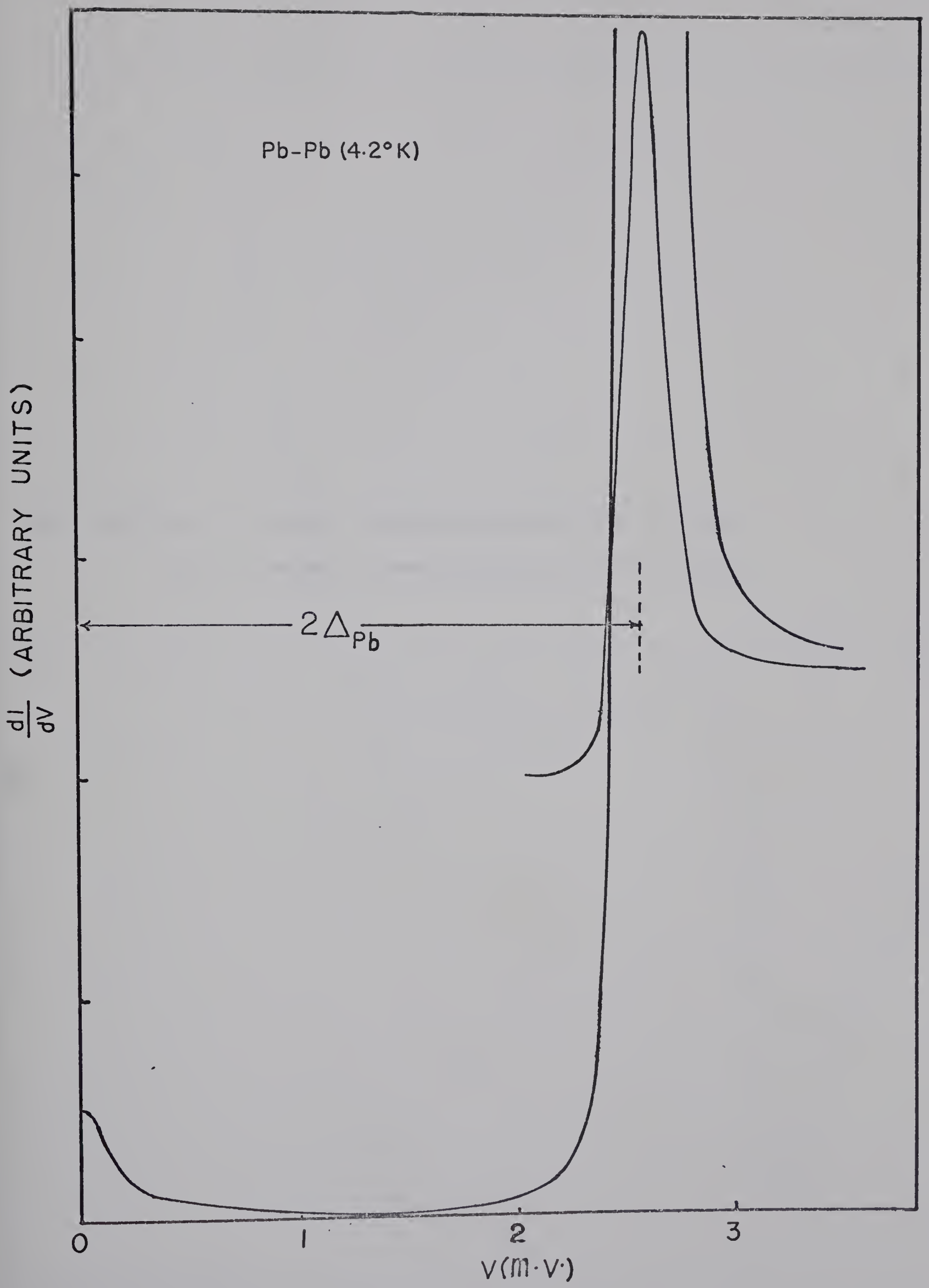
Pb-Pb (4.2°K)
$2\Delta_{Pb}$
$\frac{dI}{dV}$ (ARBITRARY UNITS)
0
1
2
3
V(m·V·)

Fig. (5-12) a) σ versus v characteristic for $0 < V \leq 10$ mv.

b) σ versus v characteristic for $10 < V \leq 30$ mv.

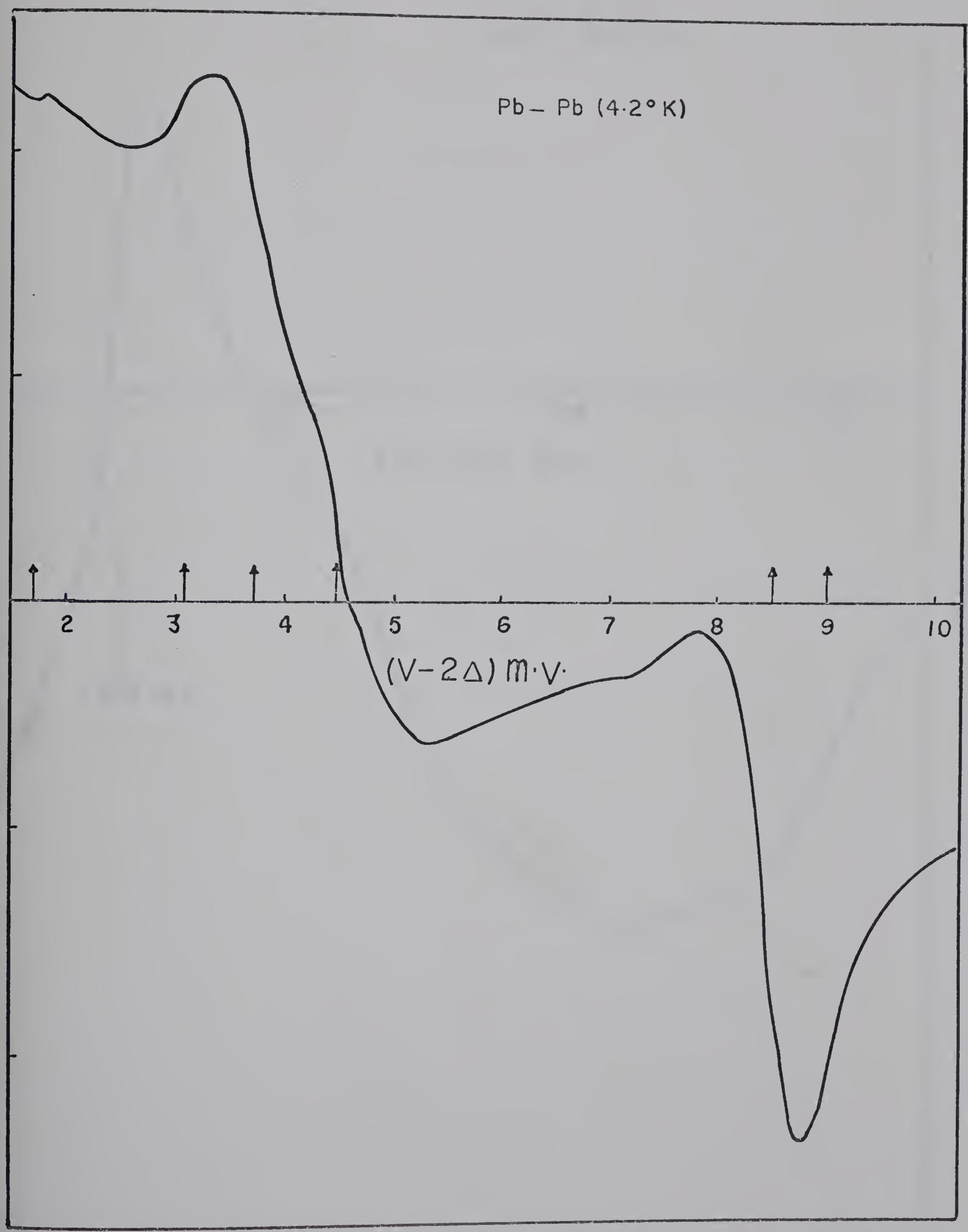
Pb – Pb (4·2° K)
(ARBITRARY UNITS)
2
3
4
5
6
7
8
9
10
(V – 2Δ) m·V·

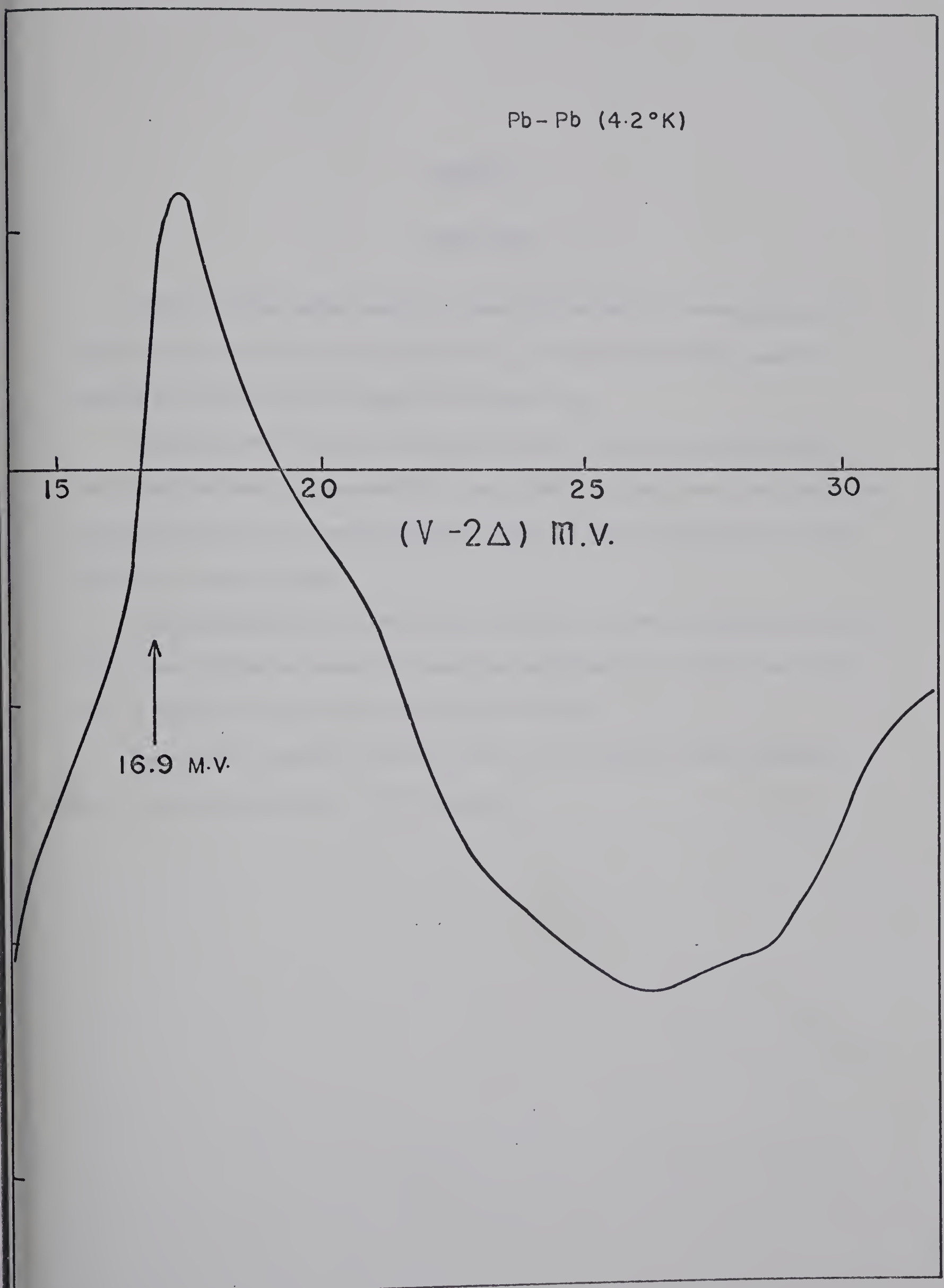
Pb – Pb (4.2°K)
15
20
25
30
(V -2Δ) M.V.
16.9 M.V.

CHAPTER 6

CONCLUSION

The tunneling techniques is a powerful method of investigating the relative jump in the specific heat at T_c, especially in the case of metals for which C_{es} is a small fraction of C_s.

Although the theories of the energy gap anisotropy predict that the relative jump in the specific heat should be less than that predicted by the BCS theory; the experimental result is not in agreement with the theories in this respect.

The discrepancies in the ratio $2\Delta(0)/KT_c$ for the same superconductor found from different electron tunneling experiments is almost certainly due to thermal stresses and anisotropy effects.

The phonon structure results for Sn and Pb are in good agreement with results published in the literature.

APPENDIX

TUNNEL JUNCTIONS AS THERMOMETERS

The current-voltage characteristics possess direct information about the temperature of the metallic films, in their superconducting states, of a tunnel junction.

At a temperature $T < T_c$°K, the thermal excited electrons and holes can tunnel from one metal to the other when a voltage $V < 2\Delta$ is applied. Rogers (1964) has calculated the normalized current $I = I_{ss}/I_{nn}$ for an applied voltage, $V = 2\overline{\Delta}$; slightly less than the energy gap 2Δ. He found that, for a symmetrical tunnel junction, the relation between the normalized current and the temperature can be written as

$$\text{A-1} \qquad I(V = 2\overline{\Delta}) = I_{ss}/I_{nn} = 1.33 \left(\frac{\Delta}{T}\right)^{\frac{1}{2}} e^{-\Delta/T} \quad .$$

Although he introduced an approximation, for the BCS function "G", in the expression of the tunnel current integral, the experimental results of our work are in good agreement with his calculation.

The observed values of I_{ss}/I_{nn} are plotted, in fig. (A-1) for two samples of Sn-Sn as a function of $\frac{\Delta(T)}{T}$ along with equation (A-1). In the same figure, other results have been obtained from one of Giaever's publications (Giaever, et al 1961) by Rogers (1964).

The discrepancy in our results may be due to small difference in energy gaps of the two tin films of the tunnel junction.

Fig. (A-1) The normalized current I_{ss}/I_{nn} versus $\frac{\Delta}{T}$ along with the mathematical expression (A-1).

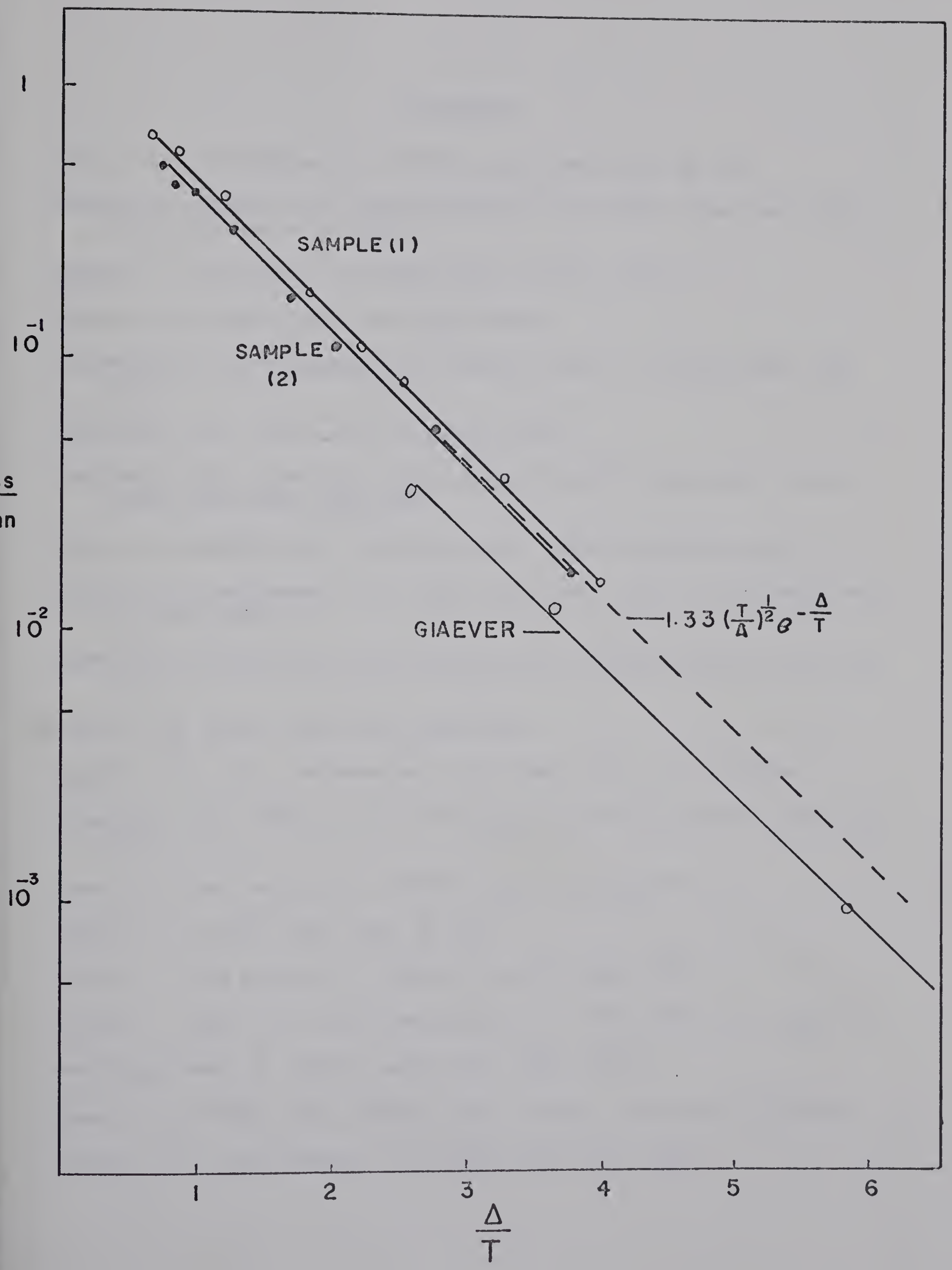
1
10^{-1}
10^{-2}
10^{-3}
$\frac{I_{ss}}{I_{nn}}$
SAMPLE (1)
SAMPLE (2)
GIAEVER
$1.33\,(\frac{T}{\Delta})^{\frac{1}{2}} e^{-\frac{\Delta}{T}}$
1
2
3
4
5
6
$\frac{\Delta}{T}$

REFERENCES

Adler, J.G., and Rogers, J.S. (1963), Phys. Rev. Lett. 10, 217.

Bardeen, J., Cooper, L.N., and Schrieffer, J.R. (1957), Phys. Rev. 108, 1175; referred to as "BCS".

Bardeen, J., and Pines, D. (1955), Phys. Rev. 99, 1140.

Bennett, A.J. (1965), Phys. Rev. 140, 1902A.

Blumberg, R.H., and Seraphin, D.P. (1962), Journal of Applied Phys. 33, 163.

Bogoliubov, N.N. (1958), Nuovo Cimento 7, 794.

Brockhouse, B.N., Arase, T., Caglioti, G., Rao, K.R., and Woods, A.D.B. (1962), Phys. Rev. 128, 1099.

Brown, A., Zemansky, M.W., and Boorse, H.A. (1953), Phys. Rev. 92, 52.

Bryant, C.A., and Keesom, P.H. (1960), Phys. Rev. Lett. 4, 460; Phys. Rev. 123, 491 (1961).

Cohen, M.H., Falicov, L.M., and Phillips, J.C. (1962), Phys. Rev. Lett. 8, 316.

Cooper, L.N. (1956), Phys. Rev. 104, 1189.

Douglass, Jr., D.H., and Meservey, R.H. (1964) Phys. Rev. 135, 19A.

Eliashberg, G.M. (1960), J.E.T.P. USSR 38, 996; Soviet physics J.E.T.P. 11 696.

Frank, J.P., and Keeler, W.J. (1967), Phys. Rev. 163, 373.

Fröhlich, H. (1950), Phys. Rev. 79, 845.

Giaever, I., and Megerle, K. (1961), Phys. Rev. 122, 1101.

Giaever, I., Hart, Jr., H.R., and Megerle, K. (1962), Phys. Rev. 126, 306.

Kamerlingh Onnes, H. (1911), Leiden Comm. 122b, 124c.

Khanna, S.M. (1965), M.Sc. Thesis, Dept. of Phys. University of Alberta.

Jennings, L.D., and Swenson, C.A. (1958), Phys. Rev. 112, 31.

Josephson, B.D. (1962), Phys. Lett. 1, 251.

Lock, J.M. (1951), Proc. Roy. Soc. (London) A208, 391.

Maxwell, E. (1950), Phys. Rev. 78, 477.

Meissner, W., and Ochsenfeld, R. (1933), Naturwiss 21, 787.

Miles, J.L., and Smith, P.H. (1963), Journal of the Electrochemical Society, 110, 1240.

Morel, P., and Anderson, P.W. (1962), Phys. Rev. 125, 1263.

Morse, R.W., and Bohm, H.V. (1957), Phys. Rev. 108, 1094.

Mühlschlegel, B. (1959), Z. Phys. 155, 313.

Pokrovskii, V.L. (1961), J.E.T.P. USSR, 40, 641; Soviet phys. J.E.T.P. 13, 447.

Pokrovskii, V.L., and Ryvkin, M.S. (1962), J.E.T.P. USSR 43, 92; Soviet phys. J.E.T.P. 16, 67 (1963).

Rogers, J.S. (1964), Ph.D. Thesis, Dept. of Phys. University of Alberta.

Rogers, J.S., Adler, J.G., and Woods, S.B. (1964), Review of Scientific Instruments 35, 208.

Rogers, J.S. (1968), "1967 Tunneling curve Tracer Manual" Dept. of Phys. University of Alberta.

Rowell, J.M., Anderson, P.W., and Thomas, D.E. (1963), Phys. Rev. Lett. 10, 334.

Rowell, J.M., and Kopf, L. (1965), Phys. Rev. 137, A902.

Schrieffer, J.R., Scalapino, D.J., and Wilkins, J.W. (1963), Phys. Rev. Lett. 10, 336.

Shepelev, A.G., and Filimonov, G.D. (1965), Soviet phys. J.E.T.P. 21, 704.

Shigi, T. (1968), Journal of the physical society of Japan, 24, 82.

Swihart, J.C. (1962), IBM Journal 6, 14.

Townsend, P., and Sutton, J. (1962), Phys. Rev. 128, 591.

Van Hove, L. (1953), Phys. Rev. 89, 1189.

Walmsley, D.G., and Campbell, C.K. (1967), Canadian Journal of Phys. 45, 1541.

Zavaritskii, N.V. (1963), J.E.T.P. 45, 1839, Soviet phys. J.E.T.P. 18, 1260, (1964).